The ELF3-BBX24/BBX25-PIF4 module controls thermosensory growth in Arabidopsis

Bidhan Chandra Malakar[1], Shivani Singh[1], Vikas Garhwal[1], Gouranga Upadhyaya[1], Rajanesh Chandramohan[1] and Sreeramaiah N. Gangappa[1,2,*]

Affiliations:

[1]Department of Biological Sciences, Indian Institute of Science Education and Research Kolkata, Mohanpur 741246, West Bengal, India

[2]Centre for Climate and Environmental Studies, Indian Institute of Science Education and Research Kolkata, Mohanpur 741246, West Bengal, India

*Author for correspondence: ngsreeram@iiserkol.ac.in (S.N.G)

The author responsible for the distribution of data and materials integral to the findings presented in this article as per the policy described in the Instructions for Authors is Sreeramaiah N. Gangappa (ngsreeram@iiserkol.ac.in)

Summary

Temperature serves as a crucial environmental cue governing the growth and adaptation of plants in their natural habitat. The B-BOX proteins play a vital role in the light-mediated regulation of growth and development. However, their role in the thermosensory signaling pathway remains poorly understood. Here, we identified two B-BOX (BBX) proteins, BBX24 and BBX25, as novel components of the thermosensory pathway to promote warm temperature-mediated growth in Arabidopsis. The *bbx24* and *bbx25* single mutants showed moderate temperature insensitivity, while the *bbx24bbx25* double mutants displayed strong temperature-insensitive hypocotyl and cotyledon growth. Warm temperatures induce *BBX24* and *BBX25* mRNA expression and protein accumulation. Genetic and biochemical analysis revealed that BBX24/BBX25 promotes thermomorphogenesis by stabilizing PHYTOCHROME INTERACTING FACTOR 4 (PIF4), a key component of the thermosensory pathway, probably through direct physical interaction. Interestingly, our study also revealed that the thermosensor EARLY FLOWERING 3 (ELF3), a potent inhibitor of PIF4 function, acts upstream of BBX24/BBX25, wherein ELF3 inhibits *BBX24/BBX25* gene expression at low ambient temperatures in the evening. However, warm temperatures render ELF3 inactive, enhancing BBX24/BBX25 activity and stabilizing PIF4 protein and thermomorphogenic growth. Together, this study unravels ELF3/BBX24/BBX25-PIF4 as a key regulatory module that controls growth and development under varying temperature cues.

Keywords: Thermomorphogenesis, BBX24, BBX25, PIF4, ELF3, gene regulation, Protein stability

Introduction

Ecological cues such as light and temperature are key in regulating plant growth, architecture, and fitness (Franklin et al., 2014; Casal and Questa, 2018; Casal and Balasubramanian, 2019; Legris et al., 2019; Lippmann et al., 2019; Quint et al.,

2023). Plants have evolved sophisticated and multifaceted mechanisms to perceive, integrate, and process these cues (Legris et al., 2019; Krahmer and Fankhauser, 2023). Because plants experience these conflicting signals in nature, they must constantly sense and integrate these signals to optimise growth and acclimatise to the local environments. However, how plants integrate and coordinate these signals is poorly understood.

Temperature has a multitude of effects on plant development (Casal and Balasubramanian, 2019; Quint et al., 2023). Specifically, warm ambient temperatures strongly influence plant growth by accelerating vegetative and reproductive transitions, resulting in shortened life-cycle duration (Koini et al., 2009; Crawford et al., 2012; Kumar et al., 2012; Casal and Balasubramanian, 2019; Krahmer and Fankhauser, 2023; Quint et al., 2023). However, warm temperatures strongly compromise immunity and also severely affect seed set and yield (Koester et al., 2014; Zhao et al., 2017; Burroughs et al., 2023). Increasing seasonal growth temperature due to global warming impairs plant growth and yield, threatening farmers' livelihood and food security (Peng et al., 2004; Zhao et al., 2017). Therefore, understanding how plants sense and integrate temperature cues is critical to delineating thermosensory signalling mechanisms to breed climate-resilient crops.

The light signaling pathway consists of photoreceptors and downstream signaling molecules that have been shown to play a pivotal role in sensing and integrating temperature cues (Li et al., 2016b; Legris et al., 2019). Key studies revealed that red-light absorbing phytochrome B (phyB) was shown to sense temperature cues (Jung et al., 2016; Legris et al., 2016). Phytochrome B exists in two interconvertible physiologically active (Pfr) and inactive (Pr) forms. Warm temperature favours the conversion of Pfr to Pr form, reducing the phyB activity (Legris et al., 2016). The phyB targets a group of growth-promoting transcription factors, PHYTOCHROME INTERACTING FACTORS (PIFs), for phosphorylation and degradation in a red-light-dependent manner (Huq and Quail, 2002; de Lucas et al., 2008b; Lorrain et al., 2008). Among PIFs, PIF4 and PIF7 have been shown to mediate

thermomorphogenesis, respectively, under SD and LD photoperiods (Koini et al., 2009; Kumar et al., 2012; Chung et al., 2020; Fiorucci et al., 2020; Burko et al., 2022; Delker et al., 2022). PIF4 is essential for warm temperature-induced hypocotyl and petiole growth, rosette development, hyponasty, and flowering (Koini et al., 2009; Kumar et al., 2012; Oh et al., 2012; Quint et al., 2016; Casal and Balasubramanian, 2019; Favero et al., 2020; Zhao and Bao, 2021; Quint et al., 2023). PIF4-mediated thermomorphogeneis is linked to the activation of genes involved in auxin/brassinosteroid biosynthesis and signaling (Franklin et al., 2011; Sun et al., 2012; Ibanez et al., 2018; Krahmer and Fankhauser, 2023), cell elongation (Gangappa and Kumar, 2017) and flowering (Kumar et al., 2012). Warm temperature-mediated inhibition of phyB activity increases PIF4 activity, resulting in the thermosensory growth (Legris et al., 2016). Unlike phyB, the blue light receptor Cryptochrome 1 (CRY1) inhibits thermomorphogenesis through PIF4 sequestration (Ma et al., 2016). Besides photoreceptors, DELLA proteins have been shown to strongly inhibit growth by interfering with PIF protein function, including PIF4, through protein degradation and sequestration (de Lucas et al., 2008a; Feng et al., 2008; Blanco-Touriñán et al., 2020). The central oscillator components of the circadian clock, including the evening complex (EC), play a crucial role in controlling thermomorphogensis by regulating PIF4 function. ELF3, a critical component of the evening complex (EC), which is also a thermosensor, inhibits *PIF4* transcription and sequesters it by forming a heterodimers (Nusinow et al., 2011; Box et al., 2015; Nieto et al., 2015; Jung et al., 2020). Pseudo-response regulators (PRRs) such as TOC1 inhibit PIF4 transcriptional capability through sequestration by forming heterodimers (Zhu et al., 2016); PRR5/7/9 inhibit PIF4 function either by inhibiting its transcription or through competitive binding to the same promoter regulatory elements such as G-box and repress its transcriptional activation of downstream genes (Zhu et al., 2016; Li et al., 2020).

Contrary to EC and PRRs, CCA1 directly promote the *PIF4* transcription and promotes the PIF4-mediated thermosensory growth (Sun et al., 2019). Moreover, upstream regulatory components such as CONSTITUTIVE PHOTOMORPHOGENIC 1 (COP1), DE-ETIOLATED 1 (DET1) and

SUPPRESSOR OF PHYTOCHROME A-105 1 (SPA1) proteins promote PIF4-mediated thermomorphogenic growth by stabilizing PIF4 protein (Gangappa and Kumar, 2017; Park et al., 2017; Lee et al., 2020). Moreover, SUPPRESSOR OF MAX2 1 (SMAX1), a karrikin signaling repressor, sequesters phyB through physical interaction and alleviates its inhibitory effect on the PIF4 transcription factor (Park et al., 2022). Recent studies also reveal that the HEMERA-REGULATOR OF the CHLOROPLAST BIOGENESIS (HMR/RCB) module works cooperatively to stabilize PIF4 during the day and promote thermomorphogenesis (Qiu et al., 2019; Qiu et al., 2021). The Heat shock transcription factor (HSF), family members, and HSFA1a/b/d/e interact with PIF4 and stabilize it during light by interfering with PIF4-phyB interaction, resulting in thermomorphogenesis during the day (Tan et al., 2023a).

The B-BOX containing zinc-finger (BBX) proteins are highly conserved transcription factors across eukaryotes that regulate gene expression by directly binding to DNA or as transcriptional co-activators or co-repressors through protein-protein interaction. BBX proteins emerged as crucial integrators of various environmental cues (Torok and Etkin, 2001; Meroni and Diez-Roux, 2005; Khanna et al., 2009; Gangappa and Botto, 2014; Ding et al., 2018; Vaishak et al., 2019; Song et al., 2020; Yuan et al., 2021). Precisely, they control seed germination, seedling photomorphogenesis, photo-pigment accumulation, flowering, and UV-B-mediated responses (Datta et al., 2008; Gangappa et al., 2013; Wang et al., 2014; Wang et al., 2015; Xu et al., 2016; Tripathi et al., 2017; Bursch et al., 2020; Song et al., 2020; Zhao et al., 2020; Job et al., 2022; Podolec et al., 2022). Moreover, their role in the shade-avoidance response, thermosensory pathway, circadian rhythm, senescence, and abiotic stress signaling is being explored (Xu et al., 2014a; Ding et al., 2018; Bai et al., 2019; Hwang et al., 2021; Yuan et al., 2021; Buelbuel et al., 2023). The BBX24 and BBX25 are close homologs that function as transcriptional co-repressors of HY5 to inhibit photomorphogenesis (Gangappa et al., 2013; Job et al., 2018). Additionally, BBX24 functions in various signaling pathways, including UV-B signaling (Jiang et al., 2012; Huang et al., 2022), shade-avoidance response (Crocco et al., 2015b; Saura-Sanchez et al., 2023) and

flowering (Li et al., 2014). However, the role of BBX24 and BBX25 in temperature-mediated regulation of growth and development remains unknown.

Here, we discovered BBX24/BBX25 as novel regulators of the thermosensory pathway and play an essential role in promoting thermomorphogenic growth. Genetic and molecular analysis revealed that *BBX24*/*BBX25* gene expression and protein levels are enhanced at warm temperatures and promote PIF4 protein stability probably through direct physical interaction, thereby promoting thermos-responsive gene expression and thermomorphogenesis. Moreover, our study demonstrates that ELF3 functions upstream of BBX24/BBX25 and inhibits their gene expression during the evening hours under low temperatures. However, warm temperature-mediated inhibition of ELF3 activity results in increased BBX24/BBX25 function and, in turn, enhances PIF4-mediated thermomorphogenic growth. Together, this study discovers ELF3-BBX24/BBX25-PIF4 as a novel regulatory module that controls thermosensory growth under dynamic temperatures.

Results

BBX24 and BBX25 are essential for warm temperature-mediated growth

To unravel the possible role of BBX24 and BBX25 in temperature-mediated regulation of hypocotyl growth, we analyzed the hypocotyl growth response of wild-type (Col-0) and *bbx24* and *bbx25* mutants grown under 22°C and 27°C. Our data revealed that *bbx24* and *bbx25* had moderate but significantly shorter hypocotyls at 22°C and 27°C than Col-0 both under short-day (SD) and long-day (LD) photoperiods (Fig. 1, A-C). Compared to Col-0, *bbx24* showed stronger inhibition in hypocotyl growth than the *bbx25* mutant at 27°C (Fig. 1, A-C). BBX24 and BBX25 function partially redundantly to promote hypocotyl growth (Gangappa et al., 2013). Consistent with this, the *bbx24bbx25* double mutant had a much shorter hypocotyl length at 27°C than the single mutants (Fig. 1, A-C), suggesting that BBX24 and BBX25 function additively in promoting warm temperature-mediated hypocotyl growth. Contrary to mutants, the *BBX24* overexpression (hereafter

referred to as *BBX24-OE*) transgenic line showed constitutive thermosensory hypocotyl growth as they had significantly longer hypocotyls than Col-0 at both 22°C and 27°C both under SD and LD (Fig. 1, D-F). To further understand whether overexpression of *BBX25* has a similar effect to *BBX24-OE* in promoting hypocotyl growth, we generated multiple transgenic lines overexpressing *BBX25* (Supplemental Fig. S1, A and B). Like *BBX24-OE* lines, transgenic lines overexpressing *BBX25* showed exaggerated hypocotyl growth compared to Col-0 at 22°C and 27°C, under SD and LD (Fig. 1, D-F, Supplemental Fig. S1, C-E). Warm temperature-mediated hypocotyl elongation is attributed to increased cell elongation, which is due to increased growth-promoting hormones such as auxin and brassinosteroid (Franklin et al., 2011; Oh et al., 2012; Ibanez et al., 2018). To know if BBX24/BBX25-mediated hypocotyl growth is due to increased cell elongation, we analyzed the cell length of hypocotyl epidermal cells from seedlings grown under 22°C and 27°C under SD. Our data reveal that the hypocotyl epidermal cell length was significantly longer in Col-0 at 27°C than at 22°C (Fig. 1G). However, in the *bbx24bbx25* double mutant, the cell length was strongly inhibited (Fig. 1G). Contrarily, *BBX24* and *BBX25* overexpression lines had significantly longer cells at both 22°C and 27°C than Col-0 (Fig. 1G). Together, these results suggest that BBX24/BBX25-mediated hypocotyl growth in response to warm temperature is linked to an increase in cell elongation of hypocotyl epidermal cells.

BBX24/BBX25 function is necessary for the thermos-responsive gene expression

To know if BBX24/BBX25 mediated thermosensory hypocotyl elongation is due to differential expression of hormone and growth-related genes, we analyzed the expression of key marker genes in response to warm temperatures. Our qRT-PCR data from SD-grown seedlings harvested at ZT23 revealed that auxin biosynthetic gene *YUCCA8* (*YUC8*), cell-wall elongation gene *XYLOGLUCAN ENDOTRANSGLYCOSYLASE 7* (*XTR7*), auxin signaling gene *INDOLE ACETIC ACID19* (*IAA19*), BR signaling gene *PACLOBUTRAZOL RESISTANCE5* (*PRE5*) showed significant downregulation in the *bbx24bbx25* mutant at 27°C, while

moderately reduced at 22°C, compared to Col-0 at corresponding temperature (Fig. 1H). However, in the *BBX24* and *BBX25* overexpression lines, these genes showed significant upregulation both at 22°C and 27°C (Fig. 1H). PIF4 directly activates many of these genes at the end of the night to promote growth. Therefore, we wanted to see if the reduced expression of these genes could be due to reduced *PIF4* transcription. Our qPCR data suggest that *PIF4* expression is moderately but significantly downregulated in the *bbx24bbx25* mutant while upregulated in *BBX24* and *BBX25* overexpression transgenic lines at the end of the night (ZT23), both at 22°C and 27°C under SD (Fig. 1H).

Additionally, our qPCR data from SD-grown seedlings harvested during daytime at ZT3 revealed that expression of growth-related genes is significantly reduced in the *bbx24bbx25* double mutant while upregulated in their respective overexpression lines at 22°C and 27°C (Supplemental Fig. S2). The *YUC8* expression in *bbx24bbx25* was significantly downregulated than Col-0 at 22°C and 27°C, while it was upregulated in the *BBX24-OE* and *BBX25-OE* lines (Supplemental Fig. S2). Similarly, BR biosynthetic gene *DWARF4* (*DWF4*) and GA biosynthetic gene *Gibberellin 3-oxidases* (*GA3OX1*) showed significant downregulation in the *bbx24bbx25* double mutant while upregulated in the overexpression lines than Col-0, at 22°C and 27C (Supplemental Fig. S2). Besides biosynthetic genes, downstream hormone signaling genes such as *IAA19*, *PRE5*, *SMALL* AUXIN *UP-REGULATED RNA 21* (*SAUR21*), and genes involved in cell elongation, such as *EXPANSIN 8* (*EXP8*) and *XTR7,* showed significant downregulation in the *bbx24bbx25* mutant (Supplemental Fig. S2, C-H), while upregulated in the *BBX24 and BBX25* overexpression lines both at 22°C and 27°C, compared to Col-0 (Supplemental Fig. S2). Together, these data confirm that BBX24/BBX25 induce the expression of growth-related genes in response to warm temperatures both at night and during the day.

BBX24/BBX25 gene expression and protein stability are enhanced in response to warm temperatures

As BBX24/BBX25 promote warm temperature-mediated hypocotyl growth, we wanted to see if warm temperature regulates their gene expression and protein stability. Our qRT-PCR data from six-day-old seedlings revealed that the expression of *BBX24* and *BBX25* showed significant upregulation at 27°C at the end of the night (ZT23) and during daytime (ZT3), compared to 22°C (Fig. 2A). Further, when we monitored the expression of *BBX24* and *BBX25* for an extended period during the day into early night, we found that *BBX24* and *BBX25* expressions peak early in the day but their expression reduced around evening and early night, both at 22°C and 27°C (Fig. 2B). Interestingly, their expression is significantly upregulated at 27°C than at 22°C (Fig. 2B). Consistent with the gene expression, immunoblot analysis of the *35S::BBX24-GFP* line revealed that BBX24 protein stability is elevated at 27°C compared to 22°C, specifically at ZT2 (Fig. 2C). Further, when we monitored BBX24 protein accumulation at different ZT time, we found that at ZT0, BBX24 protein was hardly detectable, and the protein stabilized in response to light and reached the peak at ZT2 and then reduced at ZT4 and ZT8 at 22°C (Fig. 2D). However, at 27°C, BBX24 stability increased nearly two-fold over 22°C at ZT2, and the protein level was largely comparable between 22°C and 27°C at ZT4 and ZT8 (Fig. 2D). Similarly, immunoblot analysis of the *35S::Myc-BBX25* transgenic line revealed that at ZT2, BBX25 protein stability was also elevated at 27°C compared to 22°C under SD (Fig. 2E). Specifically, BBX25 protein was more stable at ZT2 and ZT4 at 27°C compared to 22°C (Fig. 2F). Unlike BBX24, BBX25 was detectable at the end of the night (ZT23) but its stability was not altered at 27°C (Fig. 2F). Together, these results suggest that warm temperatures promote BBX24 and BBX25 accumulation both at the transcript and protein level, contributing to increased PIF4 stability.

BBX24/BBX25 promote PIF4 protein stability to facilitate thermosensory hypocotyl growth

In Arabidopsis, a bHLH transcription factor PIF4 plays a central role in promoting thermoresponsive hypocotyl growth, as *pif4-101* seedlings show strong insensitivity to warm temperature-mediated hypocotyl growth (Koini et al., 2009). Warm temperature-mediated thermosensory growth is due to a substantial increase in

PIF4 protein accumulation (Kumar et al., 2012; Gangappa and Kumar, 2017; Qiu et al., 2021). As our results above indicate that BBX24/BBX25 are required for the optimal expression of growth and hormone-related genes in response to warm temperatures, we wanted to know if this is due to differential PIF4 protein stability. Our immunoblot data from SD-grown seedlings at 22°C revealed that at the end of the night (ZT23), PIF4 protein stability was ~10-fold downregulated in the *bbx24bbx25* than Col-0 (Fig. 3A). However, during the daytime (ZT2-ZT8), PIF4 stability was decreased about two-fold in the *bbx24bbx25* compared to Col-0 at 22°C (Fig. 3A). Interestingly, at 27°C, the PIF4 stability was eight to ten folds reduced in the *bbx24bbx25* during the day (ZT2-ZT8), while approximately four folds reduced at ZT23 (Fig. 3A). However, in Col-0, PIF4 stability stayed very high at the end of the night (ZT23) and throughout the day (ZT2-ZT8) (Fig. 3A). Supporting this, when 22°C grown seedlings under SD were treated with 27°C for short durations (0, 2, 4, 8h), the PIF4 stability in Col-0 increased with the duration of warmth treatment (Fig. 3B). However, in the *bbx24bbx25*, its level stayed very low (~three to six-fold lower) than Col-0 (Fig. 3B), suggesting that the BBX24/BBX25 function is crucial for promoting PIF4 stability in response to warmth. Consistent with the role of BBX24/BBX25 in promoting PIF4 stability, overexpression of *BBX24* and *BBX25* resulted in a five to seven-fold increase in PIF4 stability at 22°C while moderate increase (~ two-folds) in PIF4 stability at 27°C (Fig. 3C), further confirming that enhanced BBX24/BBX25 activity results increased PIF4 protein accumulation. BBX24/BBX25 was shown to inhibit photomorphogenesis by interfering with the HY5 transcriptional activity (Gangappa et al., 2013). Therefore, we wanted to see if BBX24/BBX25-mediated thermosensory hypocotyl growth is due to altered HY5 protein status. Our immunoblot data suggests that HY5 protein levels were visibly reduced at 27°C than 22°C in Col-0 (Fig. 3D). However, in the *bbx24bbx25* mutant, HY5 protein level was comparable to Col-0 both at 22°C and 27°C (Fig. 3D), confirming that BBX24/BBX25-mediated thermosensory hypocotyl growth is not due to reduced HY5 levels but due to enhanced PIF4 protein accumulation.

BBX24/BBX25 mediated thermomorphogenic hypocotyl growth is linked to elevated growth hormones

Warm temperature-mediated hypocotyl growth is linked to enhanced accumulation of auxin, brassinosteroid (BR) and gibberellic acid (GA) growth hormones, which is largely mediated by PIF4 and BZR1 (Gray et al., 1998; Stavang et al., 2009; Franklin et al., 2011; Oh et al., 2012; Ibanez et al., 2018; Krahmer and Fankhauser, 2023). As BBX24/BBX25 act to promote PIF4 function, we wanted to see if BBX24/BBX25 are involved in inducing growth hormone accumulation. Our pharmacological data suggest that in response to a synthetic auxin picloram (PIC), the short hypocotyl phenotype of *bbx24bbx25* was partially recovered (Supplemental Fig. S3, A-C). The per cent (%) hypocotyl growth in the *bbx24bbx25* was comparable to Col-0 at 22°C, while at 27°C, it was significantly enhanced than Col-0 (Supplemental Fig. S3, A-C). In contrast to the *bbx24bbx25* double mutant, the *BBX24-OE* line showed enhanced sensitivity to PIC at 27°C. In comparison, the BBX25-OE line showed enhanced sensitivity both at 22°C and 27°C, compared to Col-0, as the % hypocotyl growth was significantly reduced (Supplemental Fig. S3, A-C), suggesting that BBX24/BBX25 indeed promote auxin accumulation in response warmth. Like auxin, we observed a similar response to exogenous BR (eBL, epi-brassinolide) application, wherein the hypocotyl defect is partially rescued, and % hypocotyl growth in *bbx24bbx25* double mutant was significantly enhanced than Col-0, both at 22°C and 27°C (Supplemental Fig. S3, D-F). In contrast, in the *BBX24* and *BBX25* overexpression lines, the % hypocotyl growth was significantly reduced, compared to Col-0, at 22°C and 27°C (Supplemental Fig. S3, D-F).

Moreover, our pharmacological data involving hormone inhibitors revealed that *BBX24-OE* and *BBX25-OE* transgenic lines showed enhanced sensitivity to 2,3,5-triiodobenzoic acid (TIBA, an auxin transport inhibitor) as the % hypocotyl growth was significantly reduced than Col-0 at 22°C (Supplemental Fig. S4, A-C). However, at 27°C, the *BBX24*-OE line showed significant insensitivity, while the *BBX25-OE* line showed similar sensitivity to Col-0 (Supplemental Fig. S4, A-C). Noteworthy, the % hypocotyl growth in the *BBX24-OE* and *BBX25-OE* lines at

27°C was significantly increased over 22°C, unlike Col-0, where it is reduced (Supplemental Fig. S4, A-C). These results suggest that the auxin production is probably higher in the *BBX24-OE* and *BBX25-OE* lines at 27°C, resulting in resistance to TIBA-mediated inhibition in hypocotyl growth. In response to Propiconazole (PPZ, a BR biosynthetic inhibitor), the % hypocotyl was significantly enhanced in the *BBX24-OE* at 22°C and 27°C (Supplemental Fig. S4, D-F). In contrast, the *BBX25-OE* response was comparable to Col-0 (Supplemental Fig. S4, D-F), suggesting that the rate of BR synthesis is probably higher at 22°C and 27°C in the *BBX24-OE*. These results indicate that BBX24/BBX25-mediated hypocotyl elongation in response to warm temperatures is partly due to the increased accumulation of growth hormones.

BBX24/BBX25-mediated hypocotyl elongation in response to warmth is dependent on PIF4

As BBX24/BBX25 mediated warm temperature response is linked to enhanced PIF4 protein stability, we wanted to check the genetic interaction of BBX24/BBX25 with PIF4. We introduced *pif4* mutation into *BBX24-OE* and *BBX25-OE* lines through genetic crosses and generated homozygous lines. Analysis of hypocotyl length revealed that the exaggerated hypocotyl growth of the *BBX24-OE* line was strongly suppressed in the *pif4* mutant background as the hypocotyl length of *BBX24-OE pif4* was close to the *pif4* mutant (Supplemental Fig. S5, A and B). Similarly, the *BBX25-OE pif4* hypocotyl growth was markedly suppressed compared to the *BBX25-OE* line (Supplemental Fig. S5, A and B). These results confirm that BBX24/BBX25-mediated thermosensory hypocotyl growth strongly depends on the PIF4, implying that BBX24/BBX25 probably acts upstream of PIF4.

BBX24/BBX25 function is essential for PIF4-mediated thermosensory growth

Consistent with the above results that BBX24/BBX25 are critical for maintaining PIF4 protein stability, our genetic analysis also revealed that BBX24/BBX25 are necessary for PIF4-mediated thermosensory growth (Fig. 4). While the *bbx24* or *bbx25* single mutants moderately suppressed the hypocotyl growth (Supplemental Fig. S6, A and B), the *bbx24bbx25* double mutant strongly suppressed the

exaggerated hypocotyl phenotype of *PIF4-FLAG* overexpression transgenic line (hereafter referred to as *PIF4*-OE) at 22°C and 27°C under SD (Fig. 4, A and B). Similarly, the *bbx24bbx25* double mutant showed an additive effect in suppressing the smaller cotyledon phenotype of the *PIF4-OE* line (Fig. 4, C and D), while single mutants showed a moderate but significant suppression compared to *PIF4-OE* at 22°C and 27°C under SD (Supplemental Fig. S6, C and D). Similar to SD, under LD 22°C, *bbx24* and *bbx25* mutations showed additive effects in suppressing the cotyledon phenotype of the *PIF4-OE* line (Supplemental Fig. S6, E and F). Consistent with the growth suppression, *bbx24bbx25* strongly suppressed the expression of PIF4-targeted growth-promoting genes such as *YUC8*, *IAA19*, *XTR7*, *SAUR22* and *PRE5* in the *PIF4-OE* line (Fig. 4E). Notably, in line with the reduced growth and gene expression phenotype, PIF4 protein stability was moderately reduced in the single mutants but almost undetectable in the double mutant background both at the end of the night at ZT23 (Fig. 4F) and during the day at ZT3 (Fig. 4G). Similarly, when 22°C SD grown seedlings were exposed to short-term warmth (27°C) for 24h, the PIF4 protein stability was markedly reduced in both *bbx24 PIF4-OE* and *bbx25 PIF4-OE* compared to *PIF4-OE* line while PIF4 protein was almost undetectable in the *bbx24bbx25 PIF4-OE* mutant (Fig. 4H).

In line with the role of BBX24/BBX25 in stabilizing PIF4 protein, overexpression of *BBX24* or *BBX25* in the *PIF4-OE* background, i.e., in the *PIF4-OE BBX24-OE* and *PIF4-OE BBX25-OE* double transgenic lines, the hypocotyl length was significantly increased over *PIF4-OE* (Fig. 4, I and J). Similarly, the smaller cotyledon phenotype was further exaggerated than *PIF4-OE*, specifically at 27°C (Supplemental Fig. S7, A and B). The *PIF4-OE BBX24-OE* and *PIF4-OE BBX25-OE* double overexpression transgenic lines showed etiolated growth with very long hypocotyl and half-opened or closed cotyledons, specifically at 27°C (Fig. 4, I and J), characteristic phenotype of genotypes with very high PIF4 activity. Like SD, under LD at 22°C, overexpression of *BBX24* or *BBX25* in the *PIF4-OE* background resulted in further exaggerated hypocotyl growth (Supplemental Fig. S7, C and D). Similar to the *PIF4-OE* line, the *BBX24-OE* and *BBX25-OE* lines not only showed significantly smaller cotyledons than Col-0 but also significantly enhanced the

smaller cotyledon phenotype of the *PIF4-OE* line (Supplemental Fig. S7, E and F). In line with the exaggerated growth phenotypes of the double overexpression transgenic lines, our immunoblotting data revealed that when 22°C LD grown seedlings were exposed to 27°C for 4h, PIF4 protein stability was two to three-fold elevated in the *PIF4-OE BBX24-OE* and *PIF4-OE BBX25-OE* transgenic seedlings (Fig. 4K). Collectively, these data conclude that PIF4-mediated thermosensory growth depends on BBX24/BBX25 activity.

BBX24/BBX25 physically interact with PIF4

The above results support the idea that BBX24/BBX25 are essential for stabilizing PIF4 protein at high ambient temperatures. To know if BBX24/BBX25-mediated PIF4 protein stabilization requires direct physical interactions, we carried out a Co-immunoprecipitation (Co-IP) assay. When BBX24-GFP protein was pulled down using an anti-GFP antibody, we could detect PIF4 protein in the immunoprecipitated complex using a native PIF4 antibody (Fig. 5A), while in the Col-0, which was used a negative control, we didn't detect PIF4 protein, suggesting that BBX24 physically interacts with PIF4 in vivo (Fig. 5A). Similarly, when we pulled down Myc-BBX25 using an anti-cMyc antibody, we could detect the PIF4 protein in the immunoprecipitated complex (Fig. 5B) but not when we used Col-0 as a control, implying that BBX25 physically interacts with PIF4 in vivo (Fig. 5B). Consistent with Co-IP data, Bimolecular Fluorescent Complementation (BiFC) assays from onion epidermal cells also revealed that when BBX24-nYFP/PIF4-cYFP and BBX25-nYFP/PIF4-cYFP co-transformed together, able to give a strong YFP fluorescence in the nucleus (Fig. 5C). However, BBX24-nYFP/cYFP, BBX25-nYFP/cYFP, nYFP+PIF4-cYFP and empty vector controls did not show YFP fluorescence (Fig. 5C). To further confirm these interactions, we performed yeast two-hybrid (Y2H) assays by cloning BBX24 and BBX25 with GAL4 DNA-binding domain (DBD) and PIF4 with Activation domain (AD). Our Y2H assay revealed that BBX24/PIF4 and BBX25/PIF4 co-transformed colonies were able to grow on the minimal media lacking Histidine and Adenine and were also able to activate the production of α-galactosidase, which converts 5-bromo-4-chloro-3-indolyl-beta-D-galactoside (X-α-Gal) substrate into and blue colour (Fig. 5D). However,

BBX24/AD and BBX25/AD co-transformed colonies could neither grow on minimal media lacking Histidine and Adenine nor give blue colour in the presence of X-α-Gal (Fig. 5D). Together, these shreds of evidence confirm that BBX24 and BBX25 possibly stabilize PIF4 protein through direct physical interaction.

BBX24/BBX25 inhibit DELLA protein accumulation in response to warm temperature

In Arabidopsis, DELLAs negatively regulate GA signaling to inhibit growth both by sequestering and degradation of PIF transcription factors (de Lucas et al., 2008a; Feng et al., 2008; Li et al., 2016a). BBX24 has been shown to promote PIF4-mediated SAS by inhibiting DELLA function through sequestration (Crocco et al., 2015b). Moreover, a key DELLA protein, RGA protein stability, is inhibited by warm temperatures (Blanco-Touriñán et al., 2020; Park et al., 2020). We wanted to see if BBX24/BBX25-mediated thermosensory growth is also due to altered RGA protein stability. Our immunoblotting data from six-days-old seedlings suggest that RGA protein stability is reduced at 27°C compared to 22°C in Col-0 (Supplemental Fig. S8A), as reported (Blanco-Touriñán et al., 2020; Park et al., 2020). Interestingly, the RGA protein stability was elevated in the *bbx24bbx25* double mutant than Col-0 at 22°C and 27°C (Supplemental Fig. S8A). On the contrary, RGA protein stability is strongly reduced in the overexpression lines of *BBX24* and *BBX25* compared to Col-0, both at 22°C and 27°C (Supplemental Fig. S8A). Meanwhile, qPCR data revealed that the transcript levels of *DELLA* genes were not significantly affected in the *bbx24bbx25* double mutant and the overexpression lines of *BBX24* and *BBX25* compared to Col-0 (Supplemental Fig. S8B). Together, these results indicate that BBX24/BBX25 mediate the destabilization of RGA, resulting in enhanced PIF4 function.

Further, our pharmacological data reveal that the *bbx24bbx25* double mutant grown in the presence of GA showed partial restoration of the short hypocotyl phenotype, while the *BBX24-OE* and *BBX25-OE* showed further elongated hypocotyl length (Supplemental Fig. S8C). At 22°C, the % hypocotyl growth of *bbx24bbx25* was comparable to Col-0, while the overexpression lines showed a

significant reduction in growth (Supplemental Fig. S8D). However, at 27°C, the % hypocotyl growth was significantly enhanced in the *bbx24bbx25* double mutant, while it was significantly reduced in the overexpression lines of *BBX24* and *BBX25*, compared to Col-0(Supplemental Fig. S8D). In response to Paclobutrazol (PAC, a GA biosynthesis inhibitor), *BBX24-OE* and *BBX25-OE* overexpression lines showed significant enhancement in the hypocotyl length (Supplemental Fig. 8E) and the % hypocotyl growth (Supplemental Fig. 8F) compared to Col-0, both at 22°C and 27°C. These data indicate that BBX24/BBX25-mediated hypocotyl elongation in response to warm temperatures is likely due to increased GA accumulation, leading to reduced RGA protein stability and heightened PIF4 activity and thermosensory hypocotyl growth.

ELF3 inhibits *BBX24* and *BBX25* gene expression during dawn in a temperature-dependent manner

ELF3, ELF4 and LUX ARRHYTHMO (LUX) form the Evening Complex (EC). ELF3 is the key component of EC as it bridges ELF4 and LUX (Nusinow et al., 2011) and is a critical negative regulator of thermosensory signalling (Box et al., 2015; Nieto et al., 2015; Jung et al., 2020). ELF3 strongly inhibits hypocotyl growth under optimal temperatures by directly inhibiting PIF4 transcription and its transcriptional activity through direct physical association and sequestration (Nusinow et al., 2011; Nieto et al., 2015). Our above results show that *BBX24*/*BBX25* mRNA expression peaks at the beginning of the day and is drastically reduced during the end of the day through to early night. However, their expression was significantly elevated under warm temperatures, even during the evening, as shown above (Fig. 2B). To know if ELF3 inhibits *BBX24/BBX25* gene expression in the evening, we analyzed gene expression through qPCR from Ws (Wild-type) and *elf3* seedlings harvested at ZT6 and ZT10 grown in SD. The expression of *BBX24* and *BBX25* was comparable between Ws and *elf3* mutant at ZT6 (Fig. 6, A and B). Interestingly, their expression is significantly increased in *elf3* mutant at ZT10 compared to Ws, both at 22°C and 27°C (Fig. 6, A and B), suggesting the plausible role of ELF3 in inhibiting *BBX24/BBX25* gene expression during the evening when the EC activity peaks.

LUX is a DNA-binding component of EC and has been shown to bind to conserved cis-acting variable motifs such as *AGATTCGA*, *AGATACGC*, *ATATTCGA*, *AAGATCTT* and *GGATCCGA* (Dixon et al., 2011; Nusinow et al., 2011; Chow et al., 2012; Silva et al., 2020). We looked for potential LUX binding sites to further understand if ELF3 (a component of EC) can directly bind to *BBX24* and *BBX25* promoters. Interestingly, the *BBX24* and *BBX25* promoters harbour potential LUX binding motifs, *GATACG* and *AAGATCG*, respectively (Fig. 6, C and D), which are similar to the previously reported motifs bound by LUX (Silva et al., 2020). We carried out a Chromatin Immunoprecipitation (ChIP) assay using a *35S::ELF3-YFP* transgenic line expressing stable protein at ZT10 under 22°C and 27°C under SD (Supplemental Fig. 9). Our ChIP qPCR results revealed a significant enrichment of ELF3 onto the *BBX24* and *BBX25* promoters at the region containing the LUX-Binding site in the IP samples compared to mock treatment (preimmune serum) (Fig. 6, E and F). However, the binding of ELF3 to *BBX24* and *BBX25* promoters was strongly inhibited at 27°C grown seedlings (Fig. 6, E and F). This is also consistent with the earlier reports that EC binding to the target DNA was compromised at warm temperatures (27°C) (Silva et al., 2020). In summary, our study demonstrates *BBX24*/*BBX25* as novel targets of EC for transcriptional repression at lower temperatures to inhibit growth, while warm temperature-mediated inhibition of ELF3 activity relieves this repression.

BBX24/BBX25 genetically act downstream to ELF3

To unravel if BBX24/BBX25 genetically interact with ELF3, we studied their epistatic interactions by generating *elf3bbx24* and *elf3bbx25* double mutants and *elf3bbx24bbx25* triple mutant. Measurement of hypocotyl length of double, triple and parental genotypes along with WT (segregated from Col-0xWs) suggests that while *bbx24* moderately suppressed, *bbx25* showed weaker suppression of exaggerated hypocotyl length of *elf3* (Supplemental Fig. 10, A and B). However, *bbx24bbx25* together could strongly suppress *elf3* mutant long hypocotyl phenotype as *bbx24bbx25elf3* hypocotyl length was significantly suppressed (Fig. 7, A and B). Likewise, *bbx24* and *bbx25* single mutants moderately but significantly suppressed the small cotyledon phenotype of *elf3* (Supplemental Fig. 10, C and

D), while the *bbx24bbx25* double mutants showed strong suppression of *elf3* cotyledon phenotype (Fig. 7, C and D), suggesting that *elf3* growth phenotypes are strongly dependent on BBX24/BBX25, and they plausibly act downstream to ELF3. Consistent with the suppression of growth phenotypes, our qRT-PCR data also indicates that the expression of warm temperature-induced and PIF4 target genes such as *XTR7*, *IAA19*, *PRE5* and *IAA29* was significantly downregulated in the *bbx24bbx25elf3* mutant background than *elf3,* where they are upregulated in the *elf3* mutant, compared to Col-0 (Fig. 7E).

As our genetic and molecular data reveal that BBX24/BBX25 probably function downstream to ELF3 but upstream to PIF4, we wanted to see if the suppression of *elf3* growth phenotype by *bbx24bbx25* is due to reduced PIF4 protein levels. Interestingly, our immunoblot data from six-days-old SD-grown seedlings at 22°C or 22°C-grown seedlings exposed to 27°C for 24h indeed showed that PIF4 stability is markedly reduced in the *bbx24bbx25elf3* triple mutant compared to *elf3*, both at 22°C and 27°C treated seedlings, which is comparable to *bbx24bbx25* double mutant (Fig. 7F). Moreover, increased PIF4 stability in *elf3* mutant at ZT23 and ZT8 in 22°C and 27°C grown seedlings was found to be dependent on BBX24/BBX25, as PIF4 protein stability is markedly reduced in the *bbx24bbx25elf3* triple mutant (Supplemental Fig. 10E). Together, these results confirm that BBX24/BBX25-mediated stabilization of PIF4 protein is essential for the manifestation of the *elf3* mutant growth phenotype, further reinforcing our above results that maintenance of PIF4 protein stability requires BBX24/BBX25 activity.

ELF3-BBX24/BBX25-PIF4 module controls thermosensory petiole growth and flowering

Besides hypocotyl elongation, warm temperatures promote petiole elongation and flowering, which strongly depend on PIF4 (Koini et al., 2009; Kumar et al., 2012). Consistent with the increased PIF4 activity, the *elf3* mutant shows a constitutive early flowering phenotype and has long petioles. To know if BBX24/BBX25 interfere with PIF4-mediated petiole growth and the timing of the floral transition, we analyzed the petiole length and flowering behaviour of adult plants of various

genotypes. The *PIF4-OE* and *elf3* mutant flowered early*,* as the number of rosette leaves were fewer compared to WT both under SD at 22°C and 27°C (Fig. 8, A and B) and in 22°C LD (Supplemental Fig. S11A and Fig. 8C). The *bbx24bbx25* flowered slightly but significantly later than WT (Supplemental Fig. S11B). Interestingly, *bbx24bbx25* strongly suppressed the early flowering phenotype of both *the PIF4*-OE line and *elf3* mutant, as the number of days taken to flower and the number of rosette leaves are significantly increased in the *bbx24bbx25 PIF4-OE* and *bbx24bbx25elf3* than *PIF4-OE* and *elf3,* respectively (Fig. 8, A and B), Supplemental Fig. S11B). Similarly, under LD at 22°C, *bbx24bbx25* significantly suppressed the early flowering phenotype of *PIF4-OE* and *elf3* (Supplemental Fig. S11A and B, and Fig. 8C). Moreover, *bbx24bbx25* double mutant significantly suppressed the long petiole phenotype of both the *PIF4-OE* transgenic line and *elf3* mutant at 22° and 27°C under SD and 22°C LD (Fig. 8, D and E, and Supplemental Fig. S11C). Together, these data indicate the role of BBX24/BBX25 in regulating ELF3 and PIF4-mediated petiole growth and flowering in response to varying temperatures and photoperiods.

Discussion

While increased temperatures are linked to long-day photoperiods, rising global temperatures resulting from climate change lead to increased night temperatures, profoundly affecting plant health and posing a significant threat to crop yields (Peng et al., 2004; Koester et al., 2014; Zhao et al., 2017; Burroughs et al., 2023). Plants have evolved intricate signalling mechanisms to sense, integrate, and adapt to temperature fluctuations; however, the underlying signalling mechanisms are poorly understood. As PIF4 is the central component of thermomorphogenesis, maintaining its protein stability is key to achieving optimal thermomorphogenic growth both during the night and daytime.

BBX proteins have emerged as crucial signaling nodes for orchestrating adaptive responses to diverse environmental signals such as light, shade, and abiotic and biotic stresses (Gangappa and Botto, 2014; Wang et al., 2014; Tripathi et al., 2017; Ding et al., 2018; Vaishak et al., 2019; Song et al., 2020; Zhao et al., 2020;

Podolec et al., 2022). This study reveals that BBX24/BBX25 play a positive regulatory role in temperature-responsive hypocotyl growth, irrespective of photoperiod (Fig. 1). BBX24/BBX25 functions exhibit significant overlap, as evidenced by a more pronounced reduction in cell size and hypocotyl growth in the *bbx24bbx25* double mutant than in the *bbx24* and *bbx25* single mutants at a warm temperature, as opposed to *BBX24-OE* and *BBX25-OE* overexpression lines that promoted cell elongation and hypocotyl growth (Fig. 1). Consistent with the growth phenotypes, *bbx24bbx25* double mutants had reduced expression of PIF4 target genes such as *XTR7*, *YUC8*, *EXP8*, *IAA19*, etc., involved in hormone biosynthesis and signaling both at night and during the day (Fig. 1 and Supplemental Fig. S2), which is in line with the reduced PIF4 protein stability in response to warm temperatures (Fig. 2). The enhanced thermomorphogenic response and gene expression of the *BBX24-OE* and *BBX25-OE* lines, was consistent with the increased PIF4 stability (Fig. 2). Our genetic analysis revealed that BBX24/BBX25-mediated thermomorphogenic response is directed through PIF4 (Supplemental Fig. S4). In agreement with the BBX24/BBX25 acting through PIF4, genetic analysis revealed that *bbx24* and *bbx25* strongly suppress the robust growth and gene expression phenotypes of the transgenic line overexpressing *PIF4-FLAG*, which is in line with the reduced PIF4-FLAG protein stability in the single mutants, but the complete absence of PIF4-FLAG protein in the *bbx24bbx25* background (Fig. 4). The lack of PIF4-FLAG protein was somewhat surprising compared to native PIF4 protein, and the possible reason could be the enhanced degradation of PIF4-FLAG protein over native PIF4 protein.

Several thermosensory signaling components such as HMR (HEMERA), RCB (REGULATOR OF CHLOROPLAST BIOGENESIS), and HSFA1s (HEAT SHOCK TRANSCRIPTION FACTOR 1) have been shown to stabilize PIF4 and promote daytime mediated thermomorphogenic growth (Qiu et al., 2021; Tan et al., 2023b). Meanwhile, COP1/DET1/SPA, upstream regulators of PIF4, stabilize PIF4 during the night (Gangappa and Kumar, 2017). Our study reveals that BBX24/BBX25 serve as novel upstream regulators, essential for maintaining optimal PIF4 levels at night and during the day and promoting thermomorphogenic growth (Fig. 1 and 2).

As BBX24/BBX25 and COP1/DET1 stabilize PIF4, their possible functional connection in maintaining PIF4 stability in the dark period needs further investigation. Our data suggest that PIF4 is highly unstable without BBX24/BBX25, which suggests they protect PIF4 from protein degradation machinery, probably through direct protein-protein interactions. Indeed, our protein-protein interaction data further supports this hypothesis (Fig. 5). Future research on molecular interactions with potential E3 ubiquitin ligases would address this gap. BBX24/BBX25 repress seedling photomorphogenesis by inhibiting the transcriptional activity of HY5 through physical interaction (Gangappa et al., 2013). Our data show that HY5 accumulation is barely affected by *bbx24bbx25* double mutant under 22°C and 27°C (Fig. 2D), even though HY5 stability is reduced at 27°C than 22°C in Col-0. Together, these findings suggest that BBX24/BBX25 mediated thermosensory growth is probably independent of HY5 but strongly dependent on PIF4.

DELLAs are potent repressors of the growth (de Lucas et al., 2008a; Feng et al., 2008), and regulating their protein levels is key for optimal thermomorphogenesis (Blanco-Touriñán et al., 2020; Park et al., 2020). Increased DELLAs have been shown to sequester and degrade PIF proteins, including PIF4 (Li et al., 2016a). Our data that reduced RGA protein stability seen in *BBX24-OE* and *BBX25-OE* lines but increased RGA stability in *bbx24bbx25* in response to 27°C under SD conditions suggest that BBX24/BBX25-mediated inhibition of RGA stability likely contributing to enhanced PIF4 stability. Overexpression of BBX24 does not lead to reduced RGA accumulation in response to shade (low R:FR) (Crocco et al., 2015a), while it inhibits RGA accumulation in response to warm temperatures, implying that BBX24 and possibly BBX25 regulate DELLA function through different mechanisms in a light and temperature-dependent manner.

While our study reveals that PIF4-mediated thermosensory growth depends on BBX24/BBX25, previous studies have shown that ELF3 acts upstream of PIF4 and inhibits its function to prevent elongation growth. Interestingly, our data demonstrate that the *elf3* mutant growth phenotypes, gene expression, and PIF4 protein stability strongly depend on BBX24/BBX25, suggesting that BBX24/BBX25

could act downstream to ELF3 but upstream to PIF4. Our gene expression and ChIP data further support that ELF3 inhibits *BBX24* and *BBX25* gene expression during the evening at 22°C, which is nullified at 27°C (Fig. 6), likely due to warm temperature-mediated inactivation of ELF3 activity via phase transition (Jung et al., 2020) Therefore, we propose that high PIF4 activity in *elf3* mutant is not solely attributed to the alleviation of transcriptional repression on PIF4 but due to the concurrent increase in BBX24/BBX25 activity, and these dual mechanisms together potentiate thermomorphogenic response (Fig. 7). Recently, proteins, BBX18/BBX23, shown to promote thermomorphogenic growth by inhibiting ELF3 (Ding et al., 2018). Moreover, BBX19 has also been shown to interfere with ELF3 function by forming heterodimers to regulate seedling development and flowering responses in Arabidopsis (Wang et al., 2015). Our data reveal that, unlike BBX18/BBX23, BBX24/BBX25 functions genetically downstream to ELF3, and their effect directly converges at PIF4, and elevated PIF4 protein stability in the *elf3* mutant is dependent on BBX24/BBX25 functions, further reinforcing the essential role BBX24/BBX25 in maintaining optimal PIF4 concentration to promote thermomorphogenesis. Parallelly, temperature-mediated inactivation of ELF3 results in increased *BBX24*/*BBX25* gene expression leading to enhanced protein activity at elevated temperatures, potentiating PIF4 signalling output (Fig. 7). Consistent with the role of BBX24/BBX25 in promoting PIF4 function, the PIF4-mediated thermosensory petiole growth and flowering are also dependent on PIF4 both under SD and LD photoperiods, highlighting their role beyond seedling development (Fig 8). These pieces of evidence reveal that BBX24/BBX25 proteins act as key regulators of growth and development in response to varying light and temperature cues by coordinating clock and external cues (Fig. 9). In summary, the ELF3-BBX24/BBX25-PIF4 module is critical for integrating temperature and light cues to regulate thermosensory growth and development in Arabidopsis.

Materials and methods

Plant Material and Growth Conditions

All the lines used here are in Columbia-0 (Col-0) background except *elf3*-4, which is in Wassilewskija (WS) background. The genotypes *bbx24-1*(Li et al., 2013), *bbx25-2* (Gangappa et al., 2013) *35S::BBX24-GFP* (Job et al., 2018), *pPIF4*::*PIF4-FLAG* (Gangappa et al., 2017), and *pif4-101* (Lorrain et al., 2007), *elf3-4* (Dixon and Knox 2011), and *rga-29* (Blanco-Tourinan et al., 2020) have been described previously. For hypocotyl experiments, seeds were surface sterilized with 70% ethanol containing 0.5% Triton X-100 for 10 minutes and plated on half-strength Murashige and Skoog (MS) medium (Sigma-Aldrich) supplemented with 1% sucrose, 0.5 mM MES (pH-5.7) and 0.8% agar following stratification at 4°C for four-days. For the hormone experiments, seeds were plated on MS media containing different concentrations of hormones or their inhibitors. Upon seed germination at 22°C long day (16h Light/8h Dark) growth chamber (Percival Scientific) seedlings were transferred to respective 22°C and 27°C short day (8h Light/16h Dark) conditions or as stated in the experimental conditions with 70% humidity with light intensity of 100 µmol m^{-2} sec^{-1}. Five days after germination (six-day-old), seedlings were taken for the hypocotyl length and cotyledon area measurements using ImageJ software. At least 25 seedlings for each genotype were taken for the measurements.

Bacterial and yeast strains

Escherichia coli (strains DH5a and DB3.1) and *Agrobacterium tumefaciens* (GV3101) were grown on Lysogeny broth (LB) plates or liquid media with appropriate antibiotics at 37°C and 28°C, respectively. The *Saccharomyces cerevisiae* strain, Y2H-Gold, was grown at 30°C on YPD or synthetic dropout (SD) medium with appropriate amino acid selection.

Generation of *BBX25* overexpression transgenic lines

For the generation of *35S::Myc-BBX25* overexpressing transgenic lines, the full-length BBX25 coding sequence was amplified from 22°C LD grown Col-0 cDNA and cloned into the pENTR vector through pENTR™ Directional TOPO® Cloning Kits (Invitrogen), which is then subcloned into the destination vector pGWB618 (Nakamura et al., 2010) using LR cloning kit (Invitrogen). The binary expression

cassette is then transformed into *Agrobacterium tumefaciens* GV3101 strain. Agrobacterium harbouring the transgene were transfected into Col-0 through the floral dip method. Positive transformants were selected on ½ MS containing 7.5 ug/ml glufosinate-ammonium (BASTA). Four independent lines showing 3:1 segregation on BASTA were selected for further analysis. In the T_3 generation, these lines were selected based on transgene and protein expression analysis for further analysis.

Generation of double and triple mutants

For the generation of double mutants *bbx24-1 bbx25-2*, *bbx24-1 PIF4-OE*, *bbx25-2 PIF4-OE*, *bbx24-1 pif4-101*, *bbx25-2 pif4-101*, *bbx24-1 elf3-4*, *bbx25-2 elf3-4*, *BBX24-OE PIF4-OE*, *BBX25-OE PIF4-OE* we crossed *bbx24-1* and *bbx25-2* with each other and *bbx24-1*, *bbx25-2*, *BBX24-OE* and *BBX25-OE* with the respective genotypes. For the generation of triple mutants *bbx24-1 bbx25-2 PIF4-OE* and *bbx24-1 bbx25-2 elf3-4*, we crossed homozygous double mutant *bbx24-1 PIF4-FLAG* with *bbx25-2 PIF4-FLAG* and *bbx24-1elf3-4* with *bbx25-2elf3-4* respectively. After crossing, we got F_1 seeds that grew for one more generation to get F_2 seeds. Approximately 20-30 F_2 seedlings growing on antibiotic selection were picked up where homozygosity was confirmed through PCR-based genotyping method using gene-specific and T-DNA specific primers. T-DNA-specific primers used were SALK LB1.3 for *bbx24-1*, SAIL LB3 for *pif4-101*, and *spm1* for *bbx25-2*. For *elf3-4* genotyping, we amplified PCR fragments using dCAPS primers followed by AluI restriction digestion. To confirm the homozygosity of *BBX24-OE*, *BBX25-OE*, and *PIF4-FLAG*, we first confirmed the presence of CDS using PCR, followed by survival of seedlings on antibiotic selection in the next generation. F_3 generation seedlings showing 100% survival on double antibiotic selection were used for further experiments. Primers used for genotyping are listed in Table S1.

Gene expression analysis

Approximately 100 mg seedlings from the indicated genotypes and growth conditions were harvested, frozen in liquid nitrogen, and stored at -80°C until

further processing. For RNA extraction, seedlings were ground to a fine powder in liquid nitrogen, and total RNA was isolated using an RNeasy plant mini kit (Qiagen) following the kit protocol with on-column DNase I digestion (Qiagen) for 30 min. at RT. 1.5 µg of total RNA was converted into cDNA using SuperScript® III First-Strand Synthesis kit (Invitrogen) by taking Oligo$(dT)_{20}$ primers following manufacturer's instructions. For RT-qPCR, nuclease-free water-diluted cDNA was mixed with PowerUp™ SYBR™ Green Master Mix (ThermoFisher Scientific) and gene-specific primers. Each gene RT-qPCR reaction was set in triplicate with a Biorad CFX96 Touch Real-Time PCR Detection System or an Applied Biosystems™ 7500 Fast Real-Time PCR System. The transcript level of each gene was calculated relative to that of EF1α. RT-qPCR results were analyzed in fold change using the $2^{-\Delta\Delta Ct}$ method.

Protein extraction and Immunoblotting

For western blotting, approximately 100-150 mg tissue of 6-day-old *Arabidopsis* seedlings grown in different experimental conditions were harvested in a microcentrifuge tube, snap-frozen in liquid nitrogen, and ground to fine powder in liquid nitrogen. Total protein was extracted in 250 µl of protein extraction buffer containing 50 mM Tris-HCl pH 8.0, 150 mM NaCl, 10% glycerol, 5mM DTT, 1% NP-40, 0.5mM PMSF, and 1X EDTA free Protease Inhibitor Cocktail (Roche). After resuspending in the extraction buffer, crude protein samples were cleared by centrifuging at 15,000 rpm for 10 min at 4°C. Protein concentration was estimated by Bradford reagent (Biorad). Approximately 30 µg of total protein was boiled for 5 min. at 95°C in 5x SDS gel loading dye (100 mM Tris-HCL pH 7.5, 12% glycerol, 4% SDS, 200 mM DTT, 40 mM β-ME and 0.001% bromophenol blue), separated via SDS-PAGE and transferred to the PVDF membrane (Millipore, Sigma) by wet transfer method.

For protein detection, blots were blocked with 5% skim milk in TBST for 2h at RT, incubated overnight at 4°C with respective primary antibodies, followed by incubation in 1:10,000 dilutions of horseradish peroxidase-conjugated rabbit anti-goat (Thermo Fisher Scientific, 811620) or goat anti-rabbit (Abcam, ab205718)

secondary antibodies at room temperature for 1 h. Primary antibodies were polyclonal goat anti-PIF4 antibodies (Agriseara, AS16 3955, 1:2500), polyclonal rabbit anti-GFP antibodies 1:7500 (Abcam, ab290), monoclonal HRP conjugated mouse anti-myc (HRP) antibodies (Abcam, ab62928, 1:5000), monoclonal HRP conjugated mouse anti-FLAG antibodies (Abcam, ab49763, 1:5000), polyclonal rabbit anti-HY5 antibodies (Agrisera, AS12 1867, 1:2500), Rabbit polyclonal anti-RGA antibodies, 1:2500 (Agrisera, AS11 1630), polyclonal rabbit anti-actin antibodies (Abcam, ab197345, 1:10,000), and Rabbit polyclonal anti-Histone H3 antibodies, 1:10,000 (abcam, ab1791). The chemiluminescence signal was detected using the SuperSignal West Femto kit (Thermo Fisher Scientific) and Syngene gel-doc system. Protein band intensities were measured using the ImageJ software (https://imagej.nih.gov/).

Chromatin Immunoprecipitation (ChIP)

ChIP assays were performed as previously described (Yamaguchi et al., 2014) with modifications. Approximately 1.5 g of *35S::ELF3-YFP*(*elf3-4*) seedlings grown for five days after germination at 22°C SD and 27°C SD were harvested and cross-linked with 30 ml of 1% formaldehyde in 1X PBS for 2 x 10 mins by vacuum infiltration. Crosslinking was quenched by adding 125 mM glycine under vacuum for another 5 min. Fixed seedlings were rinsed with 30 ml 1X PBS twice, dried on stacks of filter paper, frozen in liquid nitrogen and stored at -80°C. Frozen samples were crushed in liquid N_2 until they became light green and homogenized in 30 ml of extraction buffer I (10 Tris-HCL pH 8, 0.4M sucrose, 10 mM MgCl2, 5mM β-Mercaptoethanol, 2 mM PMSF and 1X protease inhibitor cocktail). Lysate was passed through 2 layers of Miracloth to remove debris and centrifuged at 1000 x g for 20 minutes at 4°C to pellet down cell organelles. Pellet resuspended in 5ml of extraction buffer II (10 mM Tris-HCL pH 8, 0.25M sucrose, 10 mM MgCl2, 1% Triton X-100, 5mM β-Mercaptoethanol, 2 mM PMSF and 1X protease inhibitor cocktail) to burst other cell organelles and centrifuged at 1000 x g for 10mins at 4°C. The deposited pellet was then dissolved in 300 µl of extraction buffer III (10 mM Tris-HCL pH 8, 1.7 M sucrose, 2mM MgCl2, 0.15% Triton X-100, 5mM β-

Mercaptoethanol, 2mM PMSF and 1X protease inhibitor cocktail) which was carefully layer at the top of 600 µl extraction buffer III and centrifuged at 16,000 x g for 1hr at 4°C to concentrate nuclei. The nuclear pellet was dissolved in 300 µl of sonication buffer, and chromatin was sheared by sonicating for 20 cycles for 30 sec. ON/OFF. Sonicated samples were cleared by centrifuging at 12000 x g for 10 mins. 1/10th of the sonicated sample was kept at -20°C as input, and the rest was diluted 10-fold in chip dilution buffer for immunoprecipitation. Protein-DNA complexes were immunoprecipitated by incubating the diluted chromatin overnight at 4°C with 15 µl of Dynabeads Protein-G (Invitrogen) equilibrated with 2 µg of anti-GFP antibody (Takara Bio, 632381). Beads were washed for 2 x 10 mins in low salt wash buffer, 1 x 10 mins in high salt wash buffer, 1 x 10 min. in LiCl wash buffer, and 2 x 10 min in TE buffer. DNA from input and IP were eluted by incubation with 10% chelax 100-resin (Biorad) at 95°C for 10mins followed by 20 µg of Proteinase K treatment at 37°C for 30 min. The supernatant was collected after centrifuging at 16000 x g for 2 min. and DNA was precipitated through the phenol-chloroform extraction method. Precipitated DNA was dissolved in 50 µl of nuclease-free water, and 2 µl was used per reaction for chip-qPCR.

Yeast two-hybrid (Y2H) assay

Y2H assay was performed following the Matchmaker® Gold Yeast Two-Hybrid System User Manual (Takara Bio). Briefly, full-length coding sequences of *BBX24* and *BBX25* were cloned into the bait vector pGBKT7 containing DNA-Binding Domain (DBD) and PIF4 into the prey vector pGADT7 having Activation Domain (AD). For checking the protein-protein interactions, different combinations of bait and prey constructs were co-transformed into Y2H Gold yeast strain (Clontech) using Yeastmaker™ Yeast Transformation kit (Clontech), and transformants were selected on double dropout medium SD/-Leu/-Trp at 30°C for three-days. For confirmation of protein-protein interactions, overnight grown double dropout screened yeast cells were diluted to an OD_{600} of 0.5 with 4X serial dilutions were spotted on quadruple dropout medium SD/-Leu/-Trp/-Ade/-His supplemented with X-alpha-gal. Plates were grown at 30°C for 72 hrs before taking the picture.

Co-Immunoprecipitation

Coimmunoprecipitation assays were performed using Dynabeads™ Protein G Immunoprecipitation Kit (Invitrogen). Approximately 500 mg of six-day-old seedlings grown at 27°C were harvested, ground in liquid nitrogen, and the powder was homogenized in 1 ml of co-immunoprecipitation buffer containing 50 mM Tris-HCL pH-8, 100 mM NaCl, 10% glycerol, 2mM DTT, 1mM EDTA, 0.1% NP-40, 1 mM PMSF, and 1X protease inhibitor cocktail. Crude protein extract was cleared by two rounds of centrifugation at 13000 rpm for 10 mins at 4°C. An aliquot of 100 µl was boiled in 5X SDS loading dye as an input. The remaining 900ul protein lysate was incubated with 50 µl Dynabeads (Invitrogen) equilibrated with anti-GFP or anti-cMyc antibody at 4°C for 6 h. Then, beads were washed, and immunoprecipitated proteins were eluted by boiling the beads at 70°C for 10 minutes in 1X Laemmli buffer. Then, input and immunoprecipitated protein samples were subjected to SDS-PAGE, and immunodetection of BBX24-GFP, Myc-BBX25 and PIF4 was accomplished using polyclonal rabbit anti-GFP (Abcam, ab290), monoclonal mouse anti-myc (Abcam, ab62928), and polyclonal goat anti-PIF4 antibodies (Agriseara AS16 3955) respectively.

Differential Interference Contrast (DIC) Microscopy for cell length measurement

For histological analysis, 6-day-old whole seedlings were fixed and cleared using serial dilution of ethanol (15%, 50%, 70%, 96% and 100%), each for 15 min in a 24-well plate. The seedlings were then kept in a cold room at 4˚ C overnight. On a subsequent day, seedlings were rehydrated in an ethanol gradient (100%, 96%, 70%, 50% and 15%), each step for 15 min., after which those were washed with 0.2 M sodium phosphate buffer (pH=7). Aniline blue (Sigma-Aldrich, Germany) staining solution was prepared as 0.1% w/v stock solution in 0.2 M sodium phosphate buffer. Seedlings were stained with a 1:20 dilution of aniline blue stock solution with 0.2M sodium phosphate buffer. Samples were incubated overnight at room temperature. Seedlings were mounted onto chloral hydrate solution (chloral hydrate: glycerol: Milli-Q water:: 8:1:2), and hypocotyls were observed using an

Olympus IX81 inverted microscope under differential interference contrast optics. Images were acquired with cellSens Standard Software (Olympus).

For each genotype, micrographs of six seedlings were obtained, and their cell length was considered under two different temperature conditions, 22°C and 27°C short-day conditions. The cell length of hypocotyls was defined as the average number of cortical cells crossing the middle portion of hypocotyls- the number of cells varies with the genotype and the growth condition. Only the cells extending in the non-dividing files were counted.

Bimolecular Fluorescent Complementation (BiFC) assay

For the BIFC assays, the *CDS* of *BBX24*, *BBX25*, and *PIF4* in the pENTR-D/TOPO vectors have been recombined into pSPYNE-nYFP and pSPYCE-cYFP vectors using LR-Clonase (Invitrogen) to obtain the fusion proteins. *BBX24* and *BBX25* were cloned into the pSPYNE vector, whereas *PIF4* was cloned in the pSPYCE vector. Sequence-verified constructs were then mobilised into *Agrobacterium tumefaciens* (strain GV3101) with the help of the freeze-thaw method. *Agrobacterium*-mediated *in planta* transient transformation onto onion bulb as reported (Xu et al., 2014b) The p19 protein of the tomato bushy stunt virus has been used to subdue gene silencing. For infiltration, nYFP-BB24/c-YFP-PIF4 and nYFP-BBX25/cYF-PIF4, along with the p19 combination, were used with a final concentration of OD_{600} 0.6: 0.6: 1.0. After infiltration, onion bulbs were kept at 28±1 °C in the dark for 72 h. The infected adaxial epidermis of the bulb scale was peeled and 29isualized with an SP8 confocal microscope (Leica, Germany) using 40X objective (ex: 488 nm for YFP, ex: 405 nm for DAPI) and deconvoluted using Leica Lightning software. Nuclei were counterstained with DAPI (1 µg/ml). A combination of nYFP-BBX24/cYFP, nYFP-BBX25/cYFP, nYFP/cYFP and nYFP/cYFP-PIF4 were used as the negative controls.

Quantification and statistical analysis

Hypocotyl length, cotyledon area, and protein band intensities were quantified using ImageJ software (https://imagej.nih.gov/). The statistically significant

difference in the data sets was analyzed using GraphPad Prism version 8.0 (https://www.graphpad.com/). One-way ANOVA or Two-way ANOVA Tukey test was used for multiple groups of observations. Students' t-test was used to determine the significance of two groups of observations. Details of the statistical analysis can be found in the figure legends.

Accession numbers

Information about the genes used in this study can be found in The Arabidopsis Information Resource database under the following accession numbers: AT1G06040 (BBX24), AT2G31380 (BBX25), AT2G43010 (PIF4), AT5G11260 (HY5), AT2G25930 (ELF3), AT2G01570 (RGA), AT4G28720 (YUC8), AT4G14130 (XTR7), AT3G15540 (IAA19), AT3G28857 (PRE5), AT3G50660 (DWF4), AT1G15550 (GA3OX1), AT1G80340 (GA3OX2), AT2G40610 (EXP8), AT5G18050 (SAUR22), AT5G18030 (SAUR21), AT4G32280 (IAA29), At3g18780 (ACT2), AT5G60390.1 (EF1α), and AT4G40030 (Histone H3.3).

Acknowledgements

We thank Prof. Salome Prat and Prof. Javier F. Botto, respectively, for sharing *35S::ELF3-YFP*(*elf3-4*) and *35S::BBX24-GFP* transgenic lines seeds. B.C.M., S.S. and V.G. acknowledge the Council of Scientific and Industrial Research, Department of Biotechnology, and University Grants Commission, respectively, for their doctoral fellowships. G.U acknowledges the Postdoctoral Fellowship from IISER Kolkata (PDF/DBS/2021/025) and Science & Engineering Research Board (SERB-PDF/2022/000529). R.C. acknowledges the KVPY Fellowship from the Department of Science and Technology, Govt. of India. We thank all the members of Gangappa lab for fruitful discussions.

Funding

This study was supported by grants from the Department of Biotechnology (Ramalingaswami Fellowship grant, BT/RLF/Re-entry/ 28/2017), Science and Engineering Research Board (Start-up Research Grant, SRG/2019/000446),

Intramural grant (IISER Kolkata), Ministry of Education (MoE/STARS-1/416) Government of India.

Author contributions

S.N.G. conceptualized, acquired funding, designed and supervised the study, analyzed data, and wrote the first and subsequent drafts of the manuscript with inputs from all the authors. B.C.M. designed the study, planned and conducted most experiments, collected results, analysed the data, and helped write the manuscript draft. S.S. planned and carried out key experiments. V.G. generated novel reagents and carried out experiments. G.U. carried out BiFC experiments. R.C. contributed to developing novel reagents. All the authors have read and approved the final version of the manuscript.

Conflict of interest statement

The authors declare that they have no conflict of interest.

References

Bai, M., Sun, J., Liu, J., Ren, H., Wang, K., Wang, Y., Wang, C., and Dehesh, K. (2019). The B-box protein BBX19 suppresses seed germination via induction of ABI5. Plant J **99,** 1192-1202.

Blanco-Tourinan, N., Legris, M., Minguet, E.G., Costigliolo-Rojas, C., Nohales, M.A., Iniesto, E., Garcia-Leomicronn, M., Pacin, M., Heucken, N., Blomeier, T., Locascio, A., Cerny, M., Esteve-Bruna, D., Diez-Diaz, M., Brzobohaty, B., Frerigmann, H., Zurbriggen, M.D., Kay, S.A., Rubio, V., Blazquez, M.A., Casal, J.J., and Alabadi, D. (2020). COP1 destabilizes DELLA proteins in Arabidopsis. Proc Natl Acad Sci U S A **117,** 13792-13799.

Blanco-Touriñán, N., Legris, M., Minguet, E.G., Costigliolo-Rojas, C., Nohales, M.A., Iniesto, E., García-León, M., Pacín, M., Heucken, N., Blomeier, T., Locascio, A., Černý, M., Esteve-Bruna, D., Díez-Díaz, M., Brzobohatý,

B., Frerigmann, H., Zurbriggen, M.D., Kay, S.A., Rubio, V., Blázquez, M.A., Casal, J.J., and Alabadí, D. (2020). COP1 destabilizes DELLA proteins in Arabidopsis. Proc Natl Acad Sci U S A **117,** 13792-13799.

Box, M.S., Huang, B.E., Domijan, M., Jaeger, K.E., Khattak, A.K., Yoo, S.J., Sedivy, E.L., Jones, D.M., Hearn, T.J., Webb, A.A.R., Grant, A., Locke, J.C.W., and Wigge, P.A. (2015). ELF3 controls thermoresponsive growth in Arabidopsis. Curr Biol **25,** 194-199.

Buelbuel, S., Sakuraba, Y., Sedaghatmehr, M., Watanabe, M., Hoefgen, R., Balazadeh, S., and Mueller-Roeber, B. (2023). Arabidopsis BBX14 negatively regulates nitrogen starvation- and dark-induced leaf senescence. Plant J **116,** 251-268.

Burko, Y., Willige, B.C., Seluzicki, A., Novák, O., Ljung, K., and Chory, J. (2022). PIF7 is a master regulator of thermomorphogenesis in shade. Nat Commun **13,** 4942.

Burroughs, C.H., Montes, C.M., Moller, C.A., Mitchell, N.G., Michael, A.M., Peng, B., Kimm, H., Pederson, T.L., Lipka, A.E., Bernacchi, C.J., Guan, K., and Ainsworth, E.A. (2023). Reductions in leaf area index, pod production, seed size, and harvest index drive yield loss to high temperatures in soybean. J Exp Bot **74,** 1629-1641.

Bursch, K., Toledo-Ortiz, G., Pireyre, M., Lohr, M., Braatz, C., and Johansson, H. (2020). Identification of BBX proteins as rate-limiting cofactors of HY5. Nature Plants **6,** 921-+.

Casal, J.J., and Questa, J.I. (2018). Light and temperature cues: multitasking receptors and transcriptional integrators. New Phytol **217,** 1029-1034.

Casal, J.J., and Balasubramanian, S. (2019). Thermomorphogenesis. Annu Rev Plant Biol **70,** 321-346.

Chow, B.Y., Helfer, A., Nusinow, D.A., and Kay, S.A. (2012). ELF3 recruitment to the PRR9 promoter requires other Evening Complex members in the Arabidopsis circadian clock. Plant Signal Behav **7,** 170-173.

Chung, B.Y.W., Balcerowicz, M., Di Antonio, M., Jaeger, K.E., Geng, F., Franaszek, K., Marriott, P., Brierley, I., Firth, A.E., and Wigge, P.A.

(2020). An RNA thermoswitch regulates daytime growth in Arabidopsis. Nat Plants **6,** 522-532.

Crawford, A.J., McLachlan, D.H., Hetherington, A.M., and Franklin, K.A. (2012). High temperature exposure increases plant cooling capacity. Curr Biol **22,** R396-397.

Crocco, C.D., Locascio, A., Escudero, C.M., Alabadí, D., Blázquez, M.A., and Botto, J.F. (2015a). The transcriptional regulator BBX24 impairs DELLA activity to promote shade avoidance in Arabidopsis thaliana. Nat Commun **6,** 6202.

Crocco, C.D., Locascio, A., Escudero, C.M., Alabadi, D., Blazquez, M.A., and Botto, J.F. (2015b). The transcriptional regulator BBX24 impairs DELLA activity to promote shade avoidance in Arabidopsis thaliana. Nat Commun **6,** 6202.

Datta, S., Johansson, H., Hettiarachchi, C., Irigoyen, M.L., Desai, M., Rubio, V., and Holm, M. (2008). LZF1/SALT TOLERANCE HOMOLOG3, an Arabidopsis B-box protein involved in light-dependent development and gene expression, undergoes COP1-mediated ubiquitination. Plant Cell **20,** 2324-2338.

de Lucas, M., Davière, J.-M., Rodríguez-Falcón, M., Pontin, M., Iglesias-Pedraz, J.M., Lorrain, S., Fankhauser, C., Blázquez, M.A., Titarenko, E., and Prat, S. (2008a). A molecular framework for light and gibberellin control of cell elongation. Nature **451,** 480-484.

de Lucas, M., Daviere, J.M., Rodriguez-Falcon, M., Pontin, M., Iglesias-Pedraz, J.M., Lorrain, S., Fankhauser, C., Blazquez, M.A., Titarenko, E., and Prat, S. (2008b). A molecular framework for light and gibberellin control of cell elongation. Nature **451,** 480-484.

Delker, C., Quint, M., and Wigge, P.A. (2022). Recent advances in understanding thermomorphogenesis signaling. Curr Opin Plant Biol **68,** 102231.

Ding, L., Wang, S., Song, Z.T., Jiang, Y., Han, J.J., Lu, S.J., Li, L., and Liu, J.X. (2018). Two B-Box Domain Proteins, BBX18 and BBX23, Interact with ELF3

and Regulate Thermomorphogenesis in Arabidopsis. Cell Rep **25,** 1718-1728 e1714.

Dixon, L.E., Knox, K., Kozma-Bognar, L., Southern, M.M., Pokhilko, A., and Millar, A.J. (2011). Temporal Repression of Core Circadian Genes Is Mediated through EARLY FLOWERING 3 in. Current Biology **21,** 120-125.

Favero, D.S., Kawamura, A., Shibata, M., Takebayashi, A., Jung, J.H., Suzuki, T., Jaeger, K.E., Ishida, T., Iwase, A., Wigge, P.A., Neff, M.M., and Sugimoto, K. (2020). AT-Hook Transcription Factors Restrict Petiole Growth by Antagonizing PIFs. Curr Biol **30,** 1454-1466 e1456.

Feng, S., Martinez, C., Gusmaroli, G., Wang, Y., Zhou, J., Wang, F., Chen, L., Yu, L., Iglesias-Pedraz, J.M., Kircher, S., Schäfer, E., Fu, X., Fan, L.-M., and Deng, X.W. (2008). Coordinated regulation of Arabidopsis thaliana development by light and gibberellins. Nature **451,** 475-479.

Fiorucci, A.S., Galvão, V.C., Ince, Y., Boccaccini, A., Goyal, A., Allenbach Petrolati, L., Trevisan, M., and Fankhauser, C. (2020). PHYTOCHROME INTERACTING FACTOR 7 is important for early responses to elevated temperature in Arabidopsis seedlings. New Phytol **226,** 50-58.

Franklin, K.A., Toledo-Ortiz, G., Pyott, D.E., and Halliday, K.J. (2014). Interaction of light and temperature signalling. J Exp Bot **65,** 2859-2871.

Franklin, K.A., Lee, S.H., Patel, D., Kumar, S.V., Spartz, A.K., Gu, C., Ye, S., Yu, P., Breen, G., Cohen, J.D., Wigge, P.A., and Gray, W.M. (2011). Phytochrome-interacting factor 4 (PIF4) regulates auxin biosynthesis at high temperature. Proc Natl Acad Sci U S A **108,** 20231-20235.

Gangappa, S.N., and Botto, J.F. (2014). The BBX family of plant transcription factors. Trends in Plant Science **19,** 460-470.

Gangappa, S.N., and Kumar, S.V. (2017). DET1 and HY5 Control PIF4-Mediated Thermosensory Elongation Growth through Distinct Mechanisms. Cell Rep **18,** 344-351.

Gangappa, S.N., Crocco, C.D., Johansson, H., Datta, S., Hettiarachchi, C., Holm, M., and Botto, J.F. (2013). The Arabidopsis B-BOX protein BBX25

interacts with HY5, negatively regulating BBX22 expression to suppress seedling photomorphogenesis. Plant Cell **25,** 1243-1257.

Gray, W.M., Ostin, A., Sandberg, G., Romano, C.P., and Estelle, M. (1998). High temperature promotes auxin-mediated hypocotyl elongation in Arabidopsis. Proc Natl Acad Sci U S A **95,** 7197-7202.

Huang, Y., Xiong, H., Xie, Y., Lyu, S., Miao, T., Li, T., Lyu, G., and Li, S. (2022). BBX24 Interacts with DELLA to Regulate UV-B-Induced Photomorphogenesis in Arabidopsis thaliana. Int J Mol Sci **23**.

Huq, E., and Quail, P.H. (2002). PIF4, a phytochrome-interacting bHLH factor, functions as a negative regulator of phytochrome B signaling in Arabidopsis. EMBO J **21,** 2441-2450.

Hwang, G., Park, J., Kim, S., Park, J., Seo, D., and Oh, E. (2021). Overexpression of BBX18 Promotes Thermomorphogenesis Through the PRR5-PIF4 Pathway. Front Plant Sci **12,** 782352.

Ibanez, C., Delker, C., Martinez, C., Burstenbinder, K., Janitza, P., Lippmann, R., Ludwig, W., Sun, H., James, G.V., Klecker, M., Grossjohann, A., Schneeberger, K., Prat, S., and Quint, M. (2018). Brassinosteroids Dominate Hormonal Regulation of Plant Thermomorphogenesis via BZR1. Curr Biol **28,** 303-310 e303.

Jiang, L., Wang, Y., Li, Q.F., Bjorn, L.O., He, J.X., and Li, S.S. (2012). Arabidopsis STO/BBX24 negatively regulates UV-B signaling by interacting with COP1 and repressing HY5 transcriptional activity. Cell Res **22,** 1046-1057.

Job, N., Lingwan, M., Masakapalli, S.K., and Datta, S. (2022). Transcription factors BBX11 and HY5 interdependently regulate the molecular and metabolic responses to UV-B. Plant Physiol **189,** 2467-2480.

Job, N., Yadukrishnan, P., Bursch, K., Datta, S., and Johansson, H. (2018). Two B-Box Proteins Regulate Photomorphogenesis by Oppositely Modulating HY5 through their Diverse C-Terminal Domains. Plant Physiol **176,** 2963-2976.

Jung, J.H., Barbosa, A.D., Hutin, S., Kumita, J.R., Gao, M., Derwort, D., Silva, C.S., Lai, X., Pierre, E., Geng, F., Kim, S.B., Baek, S., Zubieta, C., Jaeger, K.E., and Wigge, P.A. (2020). A prion-like domain in ELF3 functions as a thermosensor in Arabidopsis. Nature **585,** 256-260.

Jung, J.H., Domijan, M., Klose, C., Biswas, S., Ezer, D., Gao, M.J., Khattak, A.K., Box, M.S., Charoensawan, V., Cortijo, S., Kumar, M., Grant, A., Locke, J.C.W., Schäfer, E., Jaeger, K.E., and Wigge, P.A. (2016). Phytochromes function as thermosensors in. Science **354,** 886-889.

Khanna, R., Kronmiller, B., Maszle, D.R., Coupland, G., Holm, M., Mizuno, T., and Wu, S.H. (2009). The Arabidopsis B-box zinc finger family. Plant Cell **21,** 3416-3420.

Koester, R.P., Skoneczka, J.A., Cary, T.R., Diers, B.W., and Ainsworth, E.A. (2014). Historical gains in soybean (Glycine max Merr.) seed yield are driven by linear increases in light interception, energy conversion, and partitioning efficiencies. J Exp Bot **65,** 3311-3321.

Koini, M.A., Alvey, L., Allen, T., Tilley, C.A., Harberd, N.P., Whitelam, G.C., and Franklin, K.A. (2009). High temperature-mediated adaptations in plant architecture require the bHLH transcription factor PIF4. Curr Biol **19,** 408-413.

Krahmer, J., and Fankhauser, C. (2023). Environmental Control of Hypocotyl Elongation. Annu Rev Plant Biol.

Kumar, S.V., Lucyshyn, D., Jaeger, K.E., Alos, E., Alvey, E., Harberd, N.P., and Wigge, P.A. (2012). Transcription factor PIF4 controls the thermosensory activation of flowering. Nature **484,** 242-245.

Lee, S., Paik, I., and Huq, E. (2020). SPAs promote thermomorphogenesis by regulating the phyB-PIF4 module in Arabidopsis. Development **147**.

Legris, M., Ince, Y.C., and Fankhauser, C. (2019). Molecular mechanisms underlying phytochrome-controlled morphogenesis in plants. Nat Commun **10,** 5219.

Legris, M., Klose, C., Burgie, E.S., Rojas, C.C., Neme, M., Hiltbrunner, A., Wigge, P.A., Schafer, E., Vierstra, R.D., and Casal, J.J. (2016).

Phytochrome B integrates light and temperature signals in Arabidopsis. Science **354,** 897-900.

Li, F., Sun, J., Wang, D., Bai, S., Clarke, A.K., and Holm, M. (2014). The B-box family gene STO (BBX24) in Arabidopsis thaliana regulates flowering time in different pathways. PLoS One **9,** e87544.

Li, K., Yu, R., Fan, L.-M., Wei, N., Chen, H., and Deng, X.W. (2016a). DELLA-mediated PIF degradation contributes to coordination of light and gibberellin signalling in Arabidopsis. Nature Communications **7,** 11868.

Li, K.L., Yu, R.B., Fan, L.M., Wei, N., Chen, H.D., and Deng, X.W. (2016b). DELLA-mediated PIF degradation contributes to coordination of light and gibberellin signalling in. Nature Communications **7**.

Li, N., Zhang, Y., He, Y., Wang, Y., and Wang, L. (2020). Pseudo Response Regulators Regulate Photoperiodic Hypocotyl Growth by Repressing PIF4/5 Transcription. Plant Physiol **183,** 686-699.

Lippmann, R., Babben, S., Menger, A., Delker, C., and Quint, M. (2019). Development of Wild and Cultivated Plants under Global Warming Conditions. Curr Biol **29,** R1326-R1338.

Lorrain, S., Allen, T., Duek, P.D., Whitelam, G.C., and Fankhauser, C. (2008). Phytochrome-mediated inhibition of shade avoidance involves degradation of growth-promoting bHLH transcription factors. Plant J **53,** 312-323.

Ma, D., Li, X., Guo, Y., Chu, J., Fang, S., Yan, C., Noel, J.P., and Liu, H. (2016). Cryptochrome 1 interacts with PIF4 to regulate high temperature-mediated hypocotyl elongation in response to blue light. Proc Natl Acad Sci U S A **113,** 224-229.

Meroni, G., and Diez-Roux, G. (2005). TRIM/RBCC, a novel class of 'single protein RING finger' E3 ubiquitin ligases. Bioessays **27,** 1147-1157.

Nakamura, S., Mano, S., Tanaka, Y., Ohnishi, M., Nakamori, C., Araki, M., Niwa, T., Nishimura, M., Kaminaka, H., Nakagawa, T., Sato, Y., and Ishiguro, S. (2010). Gateway Binary Vectors with the Bialaphos Resistance Gene, as a Selection Marker for Plant Transformation. Biosci Biotech Bioch **74,** 1315-1319.

Nieto, C., Lopez-Salmeron, V., Daviere, J.M., and Prat, S. (2015). ELF3-PIF4 interaction regulates plant growth independently of the Evening Complex. Curr Biol **25,** 187-193.

Nusinow, D.A., Helfer, A., Hamilton, E.E., King, J.J., Imaizumi, T., Schultz, T.F., Farre, E.M., and Kay, S.A. (2011). The ELF4-ELF3-LUX complex links the circadian clock to diurnal control of hypocotyl growth. Nature **475,** 398-402.

Oh, E., Zhu, J.Y., and Wang, Z.Y. (2012). Interaction between BZR1 and PIF4 integrates brassinosteroid and environmental responses. Nat Cell Biol **14,** 802-809.

Park, Y.-J., Kim, J.Y., Lee, J.-H., Lee, B.-D., Paek, N.-C., and Park, C.-M. (2020). GIGANTEA Shapes the Photoperiodic Rhythms of Thermomorphogenic Growth in Arabidopsis. Molecular Plant **13,** 459-470.

Park, Y.J., Kim, J.Y., and Park, C.M. (2022). SMAX1 potentiates phytochrome B-mediated hypocotyl thermomorphogenesis. Plant Cell **34,** 2671-2687.

Park, Y.J., Lee, H.J., Ha, J.H., Kim, J.Y., and Park, C.M. (2017). COP1 conveys warm temperature information to hypocotyl thermomorphogenesis. New Phytol **215,** 269-280.

Peng, S., Huang, J., Sheehy, J.E., Laza, R.C., Visperas, R.M., Zhong, X., Centeno, G.S., Khush, G.S., and Cassman, K.G. (2004). Rice yields decline with higher night temperature from global warming. Proc Natl Acad Sci U S A **101,** 9971-9975.

Podolec, R., Wagnon, T.B., Leonardelli, M., Johansson, H., and Ulm, R. (2022). Arabidopsis B-box transcription factors BBX20-22 promote UVR8 photoreceptor-mediated UV-B responses. Plant J **111,** 422-439.

Qiu, Y., Li, M., Kim, R.J., Moore, C.M., and Chen, M. (2019). Daytime temperature is sensed by phytochrome B in Arabidopsis through a transcriptional activator HEMERA. Nat Commun **10,** 140.

Qiu, Y., Pasoreck, E.K., Yoo, C.Y., He, J., Wang, H., Bajracharya, A., Li, M., Larsen, H.D., Cheung, S., and Chen, M. (2021). RCB initiates Arabidopsis

thermomorphogenesis by stabilizing the thermoregulator PIF4 in the daytime. Nat Commun **12,** 2042.

Quint, M., Delker, C., Franklin, K.A., Wigge, P.A., Halliday, K.J., and van Zanten, M. (2016). Molecular and genetic control of plant thermomorphogenesis. Nat Plants **2,** 15190.

Quint, M., Delker, C., Balasubramanian, S., Balcerowicz, M., Casal, J.J., Castroverde, C.D.M., Chen, M., Chen, X., De Smet, I., Fankhauser, C., Franklin, K.A., Halliday, K.J., Hayes, S., Jiang, D., Jung, J.H., Kaiserli, E., Kumar, S.V., Maag, D., Oh, E., Park, C.M., Penfield, S., Perrella, G., Prat, S., Reis, R.S., Wigge, P.A., Willige, B.C., and van Zanten, M. (2023). 25 Years of thermomorphogenesis research: milestones and perspectives. Trends Plant Sci **28,** 1098-1100.

Saura-Sanchez, M., Chiriotto, T.S., Cascales, J., Gomez-Ocampo, G., Hernandez-Garcia, J., Li, Z., Pruneda-Paz, J.L., Blazquez, M.A., and Botto, J.F. (2023). BBX24 Interacts with JAZ3 to Promote Growth by Reducing DELLA Activity in Shade Avoidance. Plant Cell Physiol **64,** 474-485.

Silva, C.S., Nayak, A., Lai, X., Hutin, S., Hugouvieux, V., Jung, J.H., Lopez-Vidriero, I., Franco-Zorrilla, J.M., Panigrahi, K.C.S., Nanao, M.H., Wigge, P.A., and Zubieta, C. (2020). Molecular mechanisms of Evening Complex activity in Arabidopsis. Proc Natl Acad Sci U S A **117,** 6901-6909.

Song, Z.Q., Bian, Y.T., Liu, J.J., Sun, Y., and Xu, D. (2020). B-box proteins: Pivotal players in light-mediated development in plants. Journal of Integrative Plant Biology **62,** 1293-1309.

Stavang, J.A., Gallego-Bartolome, J., Gomez, M.D., Yoshida, S., Asami, T., Olsen, J.E., Garcia-Martinez, J.L., Alabadi, D., and Blazquez, M.A. (2009). Hormonal regulation of temperature-induced growth in Arabidopsis. Plant J **60,** 589-601.

Sun, J., Qi, L., Li, Y., Chu, J., and Li, C. (2012). PIF4-mediated activation of YUCCA8 expression integrates temperature into the auxin pathway in regulating arabidopsis hypocotyl growth. PLoS Genet **8,** e1002594.

Sun, Q., Wang, S., Xu, G., Kang, X., Zhang, M., and Ni, M. (2019). SHB1 and CCA1 interaction desensitizes light responses and enhances thermomorphogenesis. Nat Commun **10,** 3110.

Tan, W., Chen, J., Yue, X., Chai, S., Liu, W., Li, C., Yang, F., Gao, Y., Gutiérrez Rodríguez, L., Resco de Dios, V., Zhang, D., and Yao, Y. (2023a). The heat response regulators HSFA1s promote Arabidopsis thermomorphogenesis via stabilizing PIF4 during the day. Sci Adv **9,** eadh1738.

Tan, W., Chen, J., Yue, X., Chai, S., Liu, W., Li, C., Yang, F., Gao, Y., Gutierrez Rodriguez, L., Resco de Dios, V., Zhang, D., and Yao, Y. (2023b). The heat response regulators HSFA1s promote Arabidopsis thermomorphogenesis via stabilizing PIF4 during the day. Sci Adv **9,** eadh1738.

Torok, M., and Etkin, L.D. (2001). Two B or not two B? Overview of the rapidly expanding B-box family of proteins. Differentiation **67,** 63-71.

Tripathi, P., Carvallo, M., Hamilton, E.E., Preuss, S., and Kay, S.A. (2017). Arabidopsis B-BOX32 interacts with CONSTANS-LIKE3 to regulate flowering. Proc Natl Acad Sci U S A **114,** 172-177.

Vaishak, K.P., Yadukrishnan, P., Bakshi, S., Kushwaha, A.K., Ramachandran, H., Job, N., Babu, D., and Datta, S. (2019). The B-box bridge between light and hormones in plants. J Photoch Photobio B **191,** 164-174.

Wang, C.Q., Guthrie, C., Sarmast, M.K., and Dehesh, K. (2014). BBX19 interacts with CONSTANS to repress FLOWERING LOCUS T transcription, defining a flowering time checkpoint in Arabidopsis. Plant Cell **26,** 3589-3602.

Wang, C.Q., Sarmast, M.K., Jiang, J., and Dehesh, K. (2015). The Transcriptional Regulator BBX19 Promotes Hypocotyl Growth by Facilitating COP1-Mediated EARLY FLOWERING3 Degradation in Arabidopsis. Plant Cell **27,** 1128-1139.

Xu, D., Jiang, Y., Li, J., Lin, F., Holm, M., and Deng, X.W. (2016). BBX21, an Arabidopsis B-box protein, directly activates HY5 and is targeted by COP1

for 26S proteasome-mediated degradation. Proc Natl Acad Sci U S A **113,** 7655-7660.

Xu, D., Li, J., Gangappa, S.N., Hettiarachchi, C., Lin, F., Andersson, M.X., Jiang, Y., Deng, X.W., and Holm, M. (2014a). Convergence of Light and ABA signaling on the ABI5 promoter. PLoS Genet **10,** e1004197.

Xu, K., Huang, X., Wu, M., Wang, Y., Chang, Y., Liu, K., Zhang, J., Zhang, Y., Zhang, F., Yi, L., Li, T., Wang, R., Tan, G., and Li, C. (2014b). A rapid, highly efficient and economical method of Agrobacterium-mediated in planta transient transformation in living onion epidermis. PLoS One **9,** e83556.

Yamaguchi, N., Winter, C.M., Wu, M.F., Kwon, C.S., William, D.A., and Wagner, D. (2014). PROTOCOLS: Chromatin Immunoprecipitation from Arabidopsis Tissues. Arabidopsis Book **12,** e0170.

Yuan, L., Yu, Y.J., Liu, M.M., Song, Y., Li, H.M., Sun, J.Q., Wang, Q., Xie, Q.G., Wang, L., and Xu, X.D. (2021). BBX19 fine-tunes the circadian rhythm by interacting with PSEUDO-RESPONSE REGULATOR proteins to facilitate their repressive effect on morning-phased clock genes. Plant Cell **33,** 2602-2617.

Zhao, C., Liu, B., Piao, S., Wang, X., Lobell, D.B., Huang, Y., Huang, M., Yao, Y., Bassu, S., Ciais, P., Durand, J.L., Elliott, J., Ewert, F., Janssens, I.A., Li, T., Lin, E., Liu, Q., Martre, P., Muller, C., Peng, S., Penuelas, J., Ruane, A.C., Wallach, D., Wang, T., Wu, D., Liu, Z., Zhu, Y., Zhu, Z., and Asseng, S. (2017). Temperature increase reduces global yields of major crops in four independent estimates. Proc Natl Acad Sci U S A **114,** 9326-9331.

Zhao, H., and Bao, Y. (2021). PIF4: Integrator of light and temperature cues in plant growth. Plant Sci **313,** 111086.

Zhao, X., Heng, Y., Wang, X., Deng, X.W., and Xu, D. (2020). A Positive Feedback Loop of BBX11-BBX21-HY5 Promotes Photomorphogenic Development in Arabidopsis. Plant Commun **1,** 100045.

Zhu, J.Y., Oh, E., Wang, T., and Wang, Z.Y. (2016). TOC1-PIF4 interaction mediates the circadian gating of thermoresponsive growth in Arabidopsis. Nat Commun **7,** 13692.

Figures and Figure legends

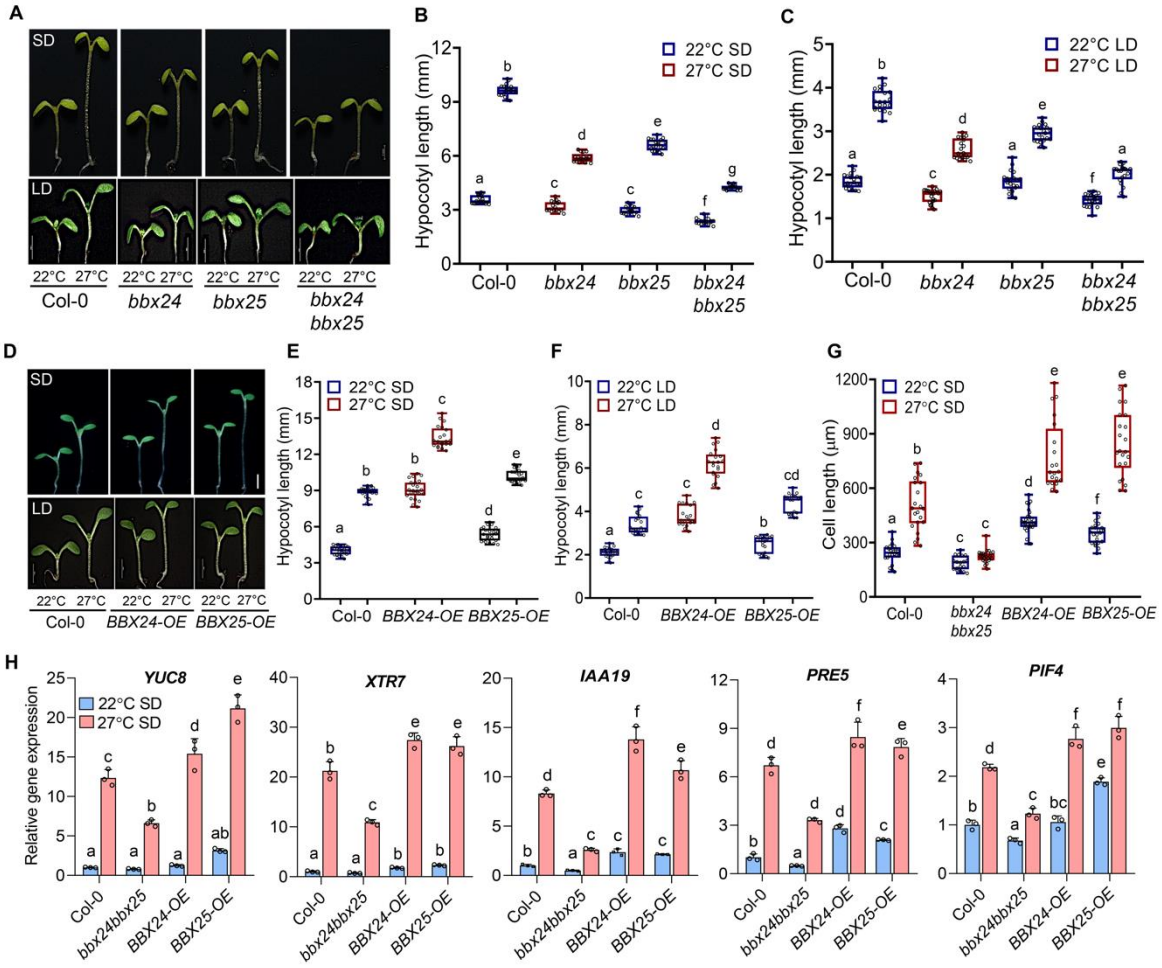

Figure 1. BBX24 and BBX25 promote thermosensory hypocotyl growth and gene expression.

(**A**) Representative images of six-day-old Col-0, *bbx24*, *bbx25*, and *bbx24bbx25* seedlings grown at 22°C and 27°C under short-day (SD, upper panel) and long-day (LD, lower panel) photoperiods.

(**B-C**) Hypocotyl length measurements (mean ± SD; n ≥ 20) of SD (B) and LD (C) grown seedlings that are shown in A.

(**D**) Representative seedling images of Col-0, *BBX24-OE*, and *BBX25-OE* (line #16) were grown at 22°C and 27°C for six days under SD (upper panel) and LD (lower panel) conditions.

(**E-F**) Hypocotyl length (mean ± SD; n ≥ 20) of SD and LD-grown seedlings shown in D.

(**G**) Cell length (mean ± SD; n ≥ 15) of hypocotyl epidermal cells from indicated genotypes grown at 22°C and 27°C for six days under SD.

(**H**) qRT-PCR analysis (mean ± SD of three biological replicates) showing relative transcript levels of thermoresponsive genes *YUC8*, *XTR7*, *IAA19*, *PRE5*, and *PIF4* in the indicated genotypes that were grown for six days at 22°C and 27°C under SD, and the samples were harvested at ZT23. *EF1α* was used as an internal control.

In A and D, the Error bars are 1 cm. In Fig. 1B,1C,1E-G, 1H-L, different letters, shown above the bars, denote statistically significant differences between the samples (Two-way ANOVA followed by Tukey's post-hoc test, $p < 0.05$). All the experiments were repeated at least two times, and similar results were obtained. In Fig. A and D, the scale bar represents 1 mm and 2 mm, respectively.

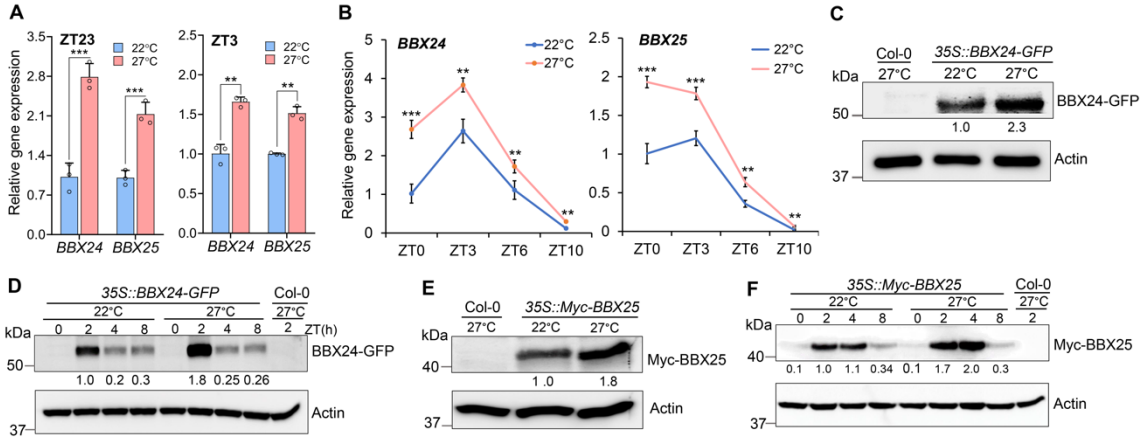

Figure 2. Warm temperatures promote BBX24/BBX25 transcript and protein accumulation.

(**A**) qRT-PCR analysis showing relative transcript levels of *BBX24* and *BBX25* from six-days-old seedlings of Col-0 grown at constant 22°C and 27°C under SD, and sampled at ZT23 and ZT3.

(**B**) qRT-PCR analysis shows *BBX24* and *BBX25* expression in six-day-old Col-0 seedlings grown at 22°C and 27°C under SD conditions, and samples were collected at indicated time points. In Fig. E-H, *EF1α* was used as a loading control, and the transcript level of each sample was normalized to Col-0 22°C or to Col-0 ZT0 time point. Error bars depict the mean ± SD of three biological replicates. Asterisks denote statistically significant differences as determined by Student's t-test, **P<0.01, ***P<0.001.

(**C** and **D**) Immunoblots showing BBX24-GFP protein level in six-days-old *35S::BBX24-GFP* seedlings grown at 22°C and 27°C under SD photoperiod and samples were harvested at ZT2 (C) or different time points as indicated (D).

(**E** and **F**) Immunoblot showing Myc-BBX25 protein status in six-days-old *35S::Myc-BBX25* seedlings grown at 22°C and 27°C under SD and samples were harvested at ZT2 (E) or different time points as indicated (F).

In Fig. C-F, 27°C grown Col-0 seedlings harvested at ZT2 were used as a negative control. Actin served as a loading control and was used for normalization. Relative protein levels (shown underneath each immunoblot) were calculated by setting 22°C grown Col-0 or 22°C grown Col-0 at ZT2 to 1. The experiments were repeated two times, and similar results were obtained.

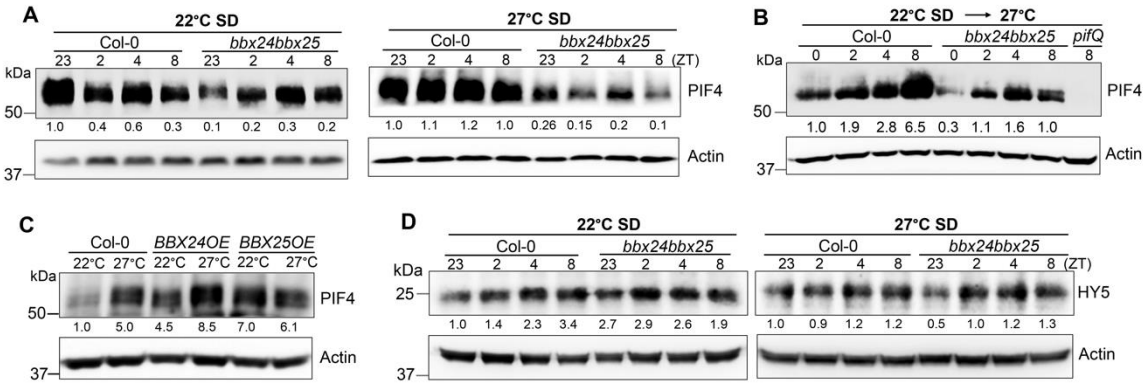
A
22°C SD
Col-0
bbx24bbx25
23 2 4 8 23 2 4 8
kDa
50
1.0 0.4 0.6 0.3 0.1 0.2 0.3 0.2
37
27°C SD
Col-0
bbx24bbx25
23 2 4 8 23 2 4 8 (ZT)
PIF4
1.0 1.1 1.2 1.0 0.26 0.15 0.2 0.1
Actin
B
22°C SD → 27°C
Col-0
bbx24bbx25
pifQ
0 2 4 8 0 2 4 8 8
kDa
50
PIF4
1.0 1.9 2.8 6.5 0.3 1.1 1.6 1.0
37
Actin
C
Col-0
BBX24OE
BBX25OE
22°C 27°C 22°C 27°C 22°C 27°C
kDa
50
PIF4
1.0 5.0 4.5 8.5 7.0 6.1
37
Actin
D
22°C SD
Col-0
bbx24bbx25
23 2 4 8 23 2 4 8
kDa
25
1.0 1.4 2.3 3.4 2.7 2.9 2.6 1.9
37
27°C SD
Col-0
bbx24bbx25
23 2 4 8 23 2 4 8 (ZT)
HY5
1.0 0.9 1.2 1.2 0.5 1.0 1.2 1.3
Actin

Figure 3. BBX24/BBX25 promotes thermosensory growth by stabilizing PIF4 transcription factor.

(**A**) Immunoblot analysis of PIF4 protein levels in six-day-old Col-0 and *bbx24bbx25* seedlings grown diurnally at 22°C and 27°C under SD and samples were harvested at the indicated time (ZT) points.

(**B**) Immunoblot showing PIF4 protein levels in Col-0 and *bbx24bbx25* double mutant seedlings grown at 22°C SD for six days or 22°C SD grown seedlings exposed to 27°C for indicated time points. The *pifQ* mutant was used as a negative control.

(**C**) Immunoblot analysis of PIF4 protein level in six-day-old Col-0, *BBX24-OE*, and *BBX25-OE* seedlings grown at constant 22°C and 27°C under SD photoperiod, and tissue was harvested at ZT23.

(**D**) Immunoblot analysis of HY5 protein levels in six-day-old Col-0 and *bbx24bbx25* seedlings grown diurnally at 22°C and 27°C under SD and sampled at the indicated time (ZT) points.

In A-D, Actin was used as a loading control. The normalized PIF4 protein level in Col-0 at ZT0 was set to 1, and others are calculated relative to Col-0 and shown underneath each immunoblot.

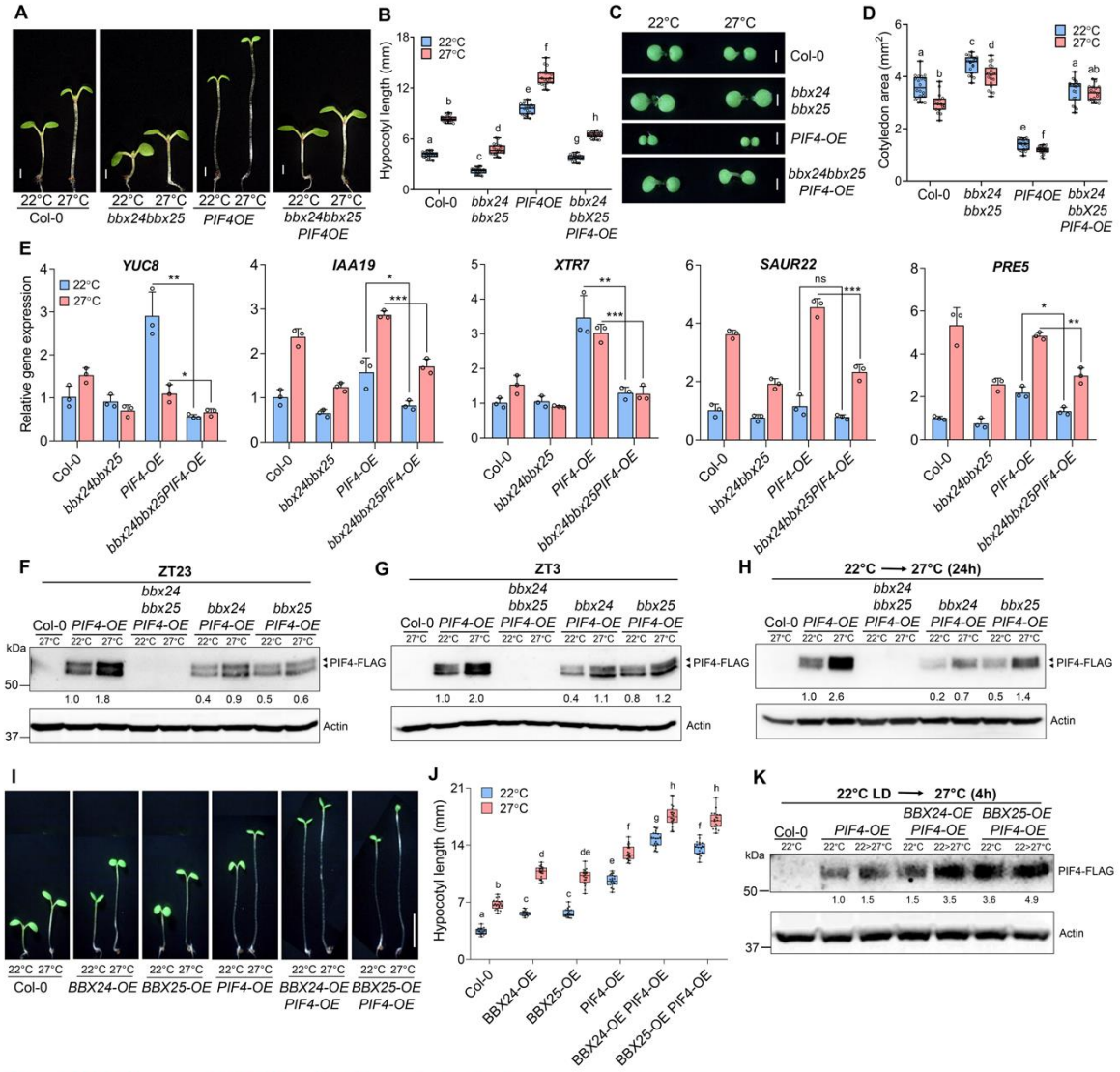

Figure 4. BBX24/BBX25 are essential for PIF4-mediated hypocotyl elongation in response to warm ambient temperatures.

(**A**) Representative seedling images of six-days-old Col-0*, bbx24bbx25, PIF4-OE*, and *bbx24bbx25PIF4-OE* seedlings grown at 22°C and 27°C under SD.

(**B**) Hypocotyl length (mean ± SD; n ≥ 20) of seedlings shown in A.

(**C** and **D**) Representative cotyledon images (C) and cotyledon area (mean ± SD; n ≥ 20) (D) of six-day-old indicated genotypes grown at 22°C and 27°C under SD.

(**E**) qRT-PCR analysis showing relative transcript level (normalized to 22°C Col-0) of PIF4 target genes *YUC8*, *XTR7*, *SAUR22* and *PRE5* from six-days-old indicated genotypes grown at 22°C and 27°C under SD, sampled ZT23. *EF1α* was used as

an internal control, Error bars depict the mean ± SD of three biological replicates. Asterisks denote statistically significant differences (Student's t-test, *P<0.05, **P<0.01, ***P<0.001) between indicated pairs of genotypes under respective temperatures.

(**F-H**) Immunoblot analysis of PIF4-FLAG protein levels in indicated genotypes grown for six days at 22°C and 27°C, and samples are harvested at ZT23 (F) or ZT3 (G) or 22°C SD grown five-day-old seedlings shifted to 27°C for 24h and sampled at ZT23 (H). Col-0 was used as a negative control. The relative PIF4 protein levels were normalized against Actin and are shown underneath each immunoblot. The normalized PIF4 in PIF4-OE at 22°C short day conditions was set to 1, and others were calculated as relative levels. We detected two bands of PIF4-FLAG, and the top band probably corresponds to the phosphorylated form of PIF4.

(**I** and **J**) Representative seedling images (I) and hypocotyl length (mean ± SD; n ≥ 20) (J) of six-day-old various genotypes, as mentioned, grown at 22°C and 27°C under SD. Different letters denote statistically significant differences between the samples as determined by Two-way ANOVA followed by Tukey's post-hoc test, $p < 0.05$).

(**K**) Immunoblot showing PIF4-FLAG protein levels in indicated genotypes grown for five days at 22°C long day or shifted to 27°C for 4 h. Col-0 was used as a negative control. Actin was used for normalization. The relative PIF4-FLAG protein levels were calculated against Col-0 22°C, set to 1.

The scale bar represents in Fig. A and C represents 1 mm and in Fig. I, the scale bar = 2 mm. The experiments were repeated at least two times, and similar results were obtained.

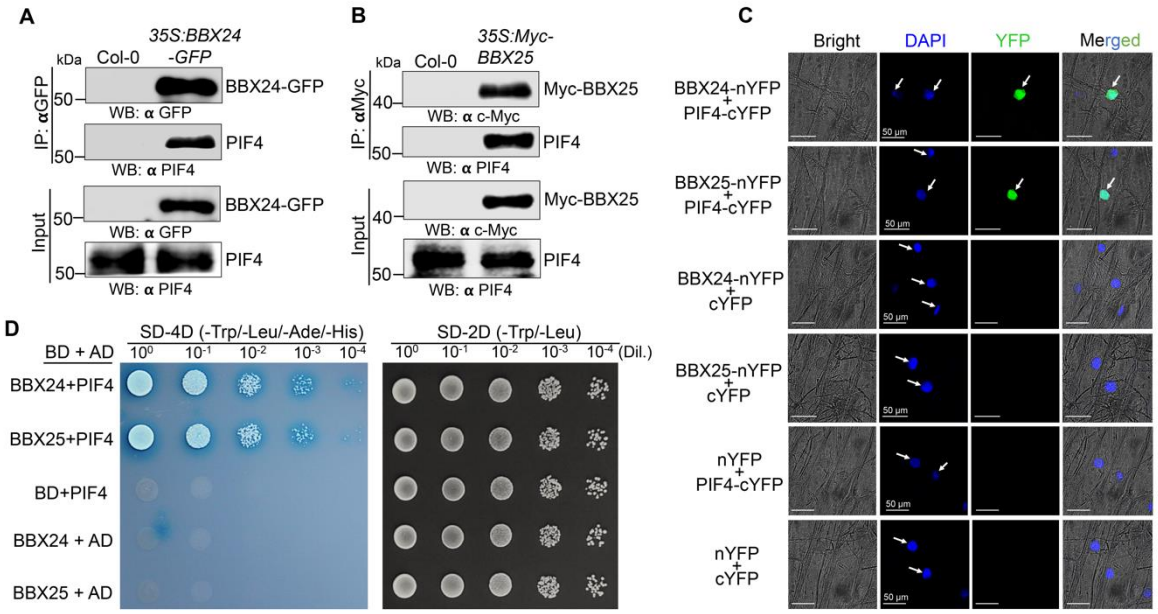

Figure 5. BBX24/BBX25 physically interact with PIF4 in-vivo.

(**A**) Immunoblots of coimmunoprecipitation assays showing BBX24 interacts with PIF4 in planta. Total protein from six-day-old Col-0 and *35S::BBX24-GFP* seedlings grown at 27°C, sampled at ZT2, were used, and BBX24-GFP was pulled down using anti-GFP antibody coupled to magnetic Dynabeads. BBX24-GFP and PIF4 from input and pulldown fractions were detected by immunoblot using anti-GFP and native anti-PIF4 antibodies.

(**B**) Immunoblots of coimmunoprecipitation assay showing BBX25 interacts with PIF4 in planta. Total protein from six-day-old Col-0 and *35S::Myc-BBX25* seedlings grown at 27°C, sampled at ZT2, were used, and Myc-BBX25 was immunoprecipitated using an anti-myc antibody coupled to magnetic Dynabeads. Myc-BBX25 and PIF4 from input and pulldown fractions were detected by immunoblotting using anti-Myc and native anti-PIF4 antibodies.

(**C**) BiFC assays show the physical interaction of BBX24 and BBX25 with PIF4 in planta in onion epidermal cells. The adaxial epidermis of the onion bulb was co-infiltrated with nYFP, BBX24-nYFP, or BBX25-nYFP, and cYFP or PIF4-cYFP as indicated. Two days after incubation, onion peels were analysed for fluorescence in different combinations of co-infiltered samples. All the interactions were repeated twice, and similar results were observed.

(**D**) BBX24 and BBX25 physically interact with PIF4 in yeast. Overnight grown cultures of Y2H Gold yeast strain containing different combinations of bait (pGBKT7, pGBKT7-BBX24, and pGBKT7-BBX25) and prey (pGADT7 and pGADT7-PIF4) constructs diluted to an OD_{600} of 0.5 with 4x serial dilutions were spotted on double and quadruple dropout medium supplemented with X-alpha-gal. Pictures were taken after 72 h of incubation at 30°C.

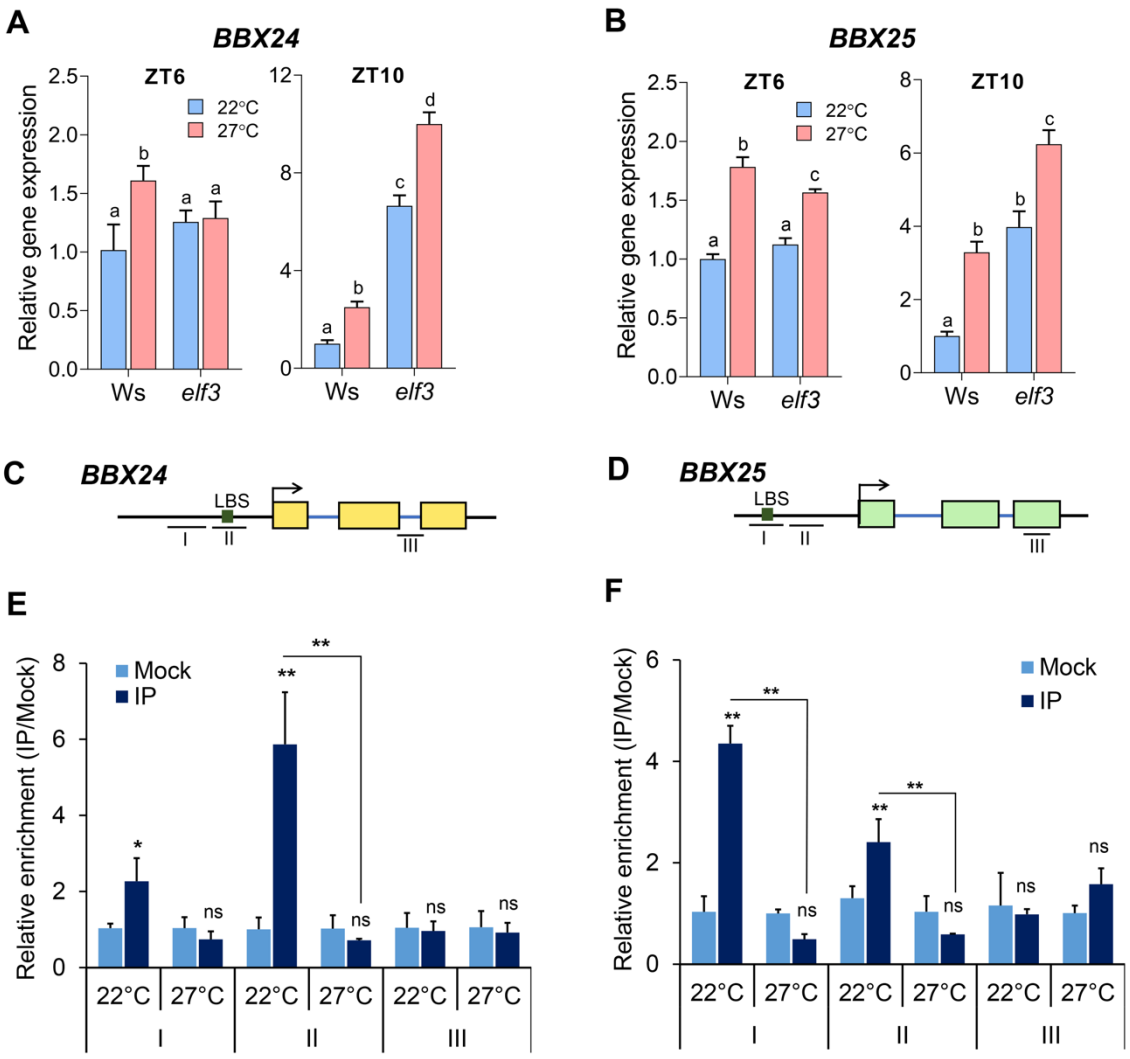

Figure 6. ELF3 represses *BBX24*/*BBX25* transcription during dawn while warm temperature dampens it.

(**A** and **B**) qRT-PCR analysis showing relative transcript levels of *BBX24* and *BBX25* in six-day-old seedlings of Ws and *elf3* grown at constant 22°C and 27°C SD conditions, sampled at ZT6 and ZT10. The expression level of each sample was normalized to Ws at 22°C of the respective time point, which was normalized to that of *EF1α*. The data shown is the mean ± SD, with Error bars depicting SD (n=3 biological replicates).

(**C** and **D**) Schematic representation of *BBX24* and *BBX25* promoters depicting LUX binding sites and the exact position of each PCR fragment used for analysis.

(**E** and **F**) ChIP-qPCR assay showing ELF3 enrichment onto *BBX24* and *BBX25* promoters in vivo. Seedlings of *35S::ELF3-YFP* (*elf3-4*) were grown at 22°C and 27°C SD conditions for five days after germination and sampled at ZT10 for crosslinking. For each amplicon, fold enrichment was calculated as a ratio between anti-GFP and mock (pre-immune serum). Genomic fragment towards the *3'UTR* of *BBX24* and *BBX25* was used as a negative control. The data shown is the (mean ± SD, n=2, two biological replicates. The experiment was repeated twice, and similar results were seen. Asterisks denote statistically significant differences as determined by Student's t-test, *P<0.05, **P<0.01.

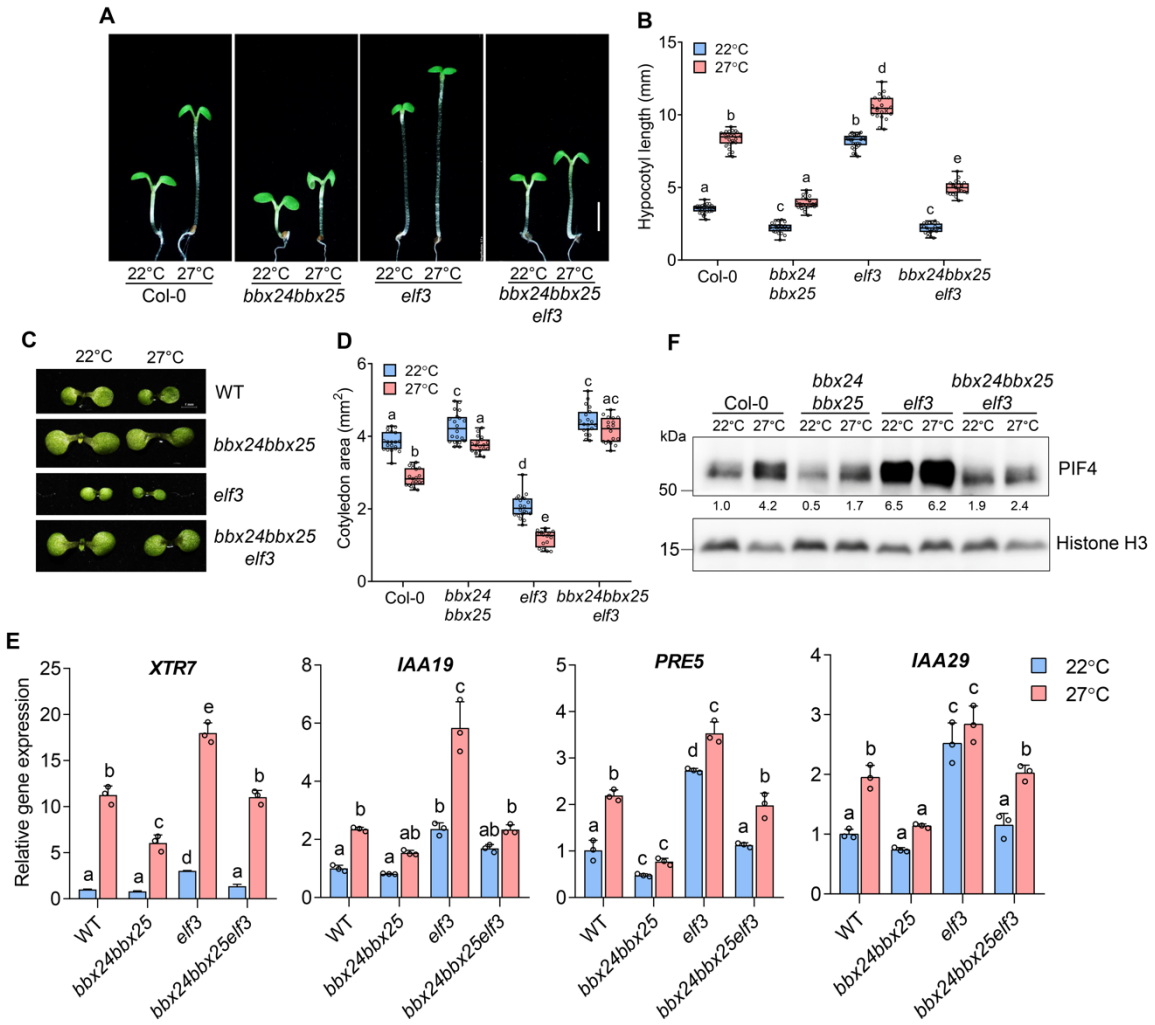

Figure 7. ELF3 genetically interact with BBX24/BBX25 to repress PIF4-mediated thermosensory growth.

(**A** and **B**) Representative seedling images (A) and hypocotyl length (B), of six-day-old segregated WT (Col-0xWs), *bbx24bbx25*, *elf3*, *bbx24elf3*, *bbx25elf3* and *bbx24bbx25elf3* seedlings grown at 22°C and 27°C under SD. In Fig. E, the scale bar represents 1 mm.

(**C** and **D**) Representative cotyledon images (C) and cotyledon area (D) of indicated genotypes shown in A, grown at 22°C and 27°C under SD. In Fig. C, the scale bar represents 1 mm.

(**E**) qRT-PCR data shows transcript level of *IAA19*, *XTR7*, and *PRE5* in six-day-old indicated genotypes at 22°C and 27°C under SD and tissue was harvested at ZT3.

EF1α was used as an internal control, and the transcript level of each sample was normalized against WT 22°C SD. In Fig. A, B, and F-J, different letters denote statistically significant differences between the samples as analyzed through Two-way ANOVA followed by Tukey's post-hoc test, $p < 0.05$).

(**F**) Immunoblots showing PIF4 protein levels in WT (Col-0xWs), *bbx24bbx25*, *elf3* and *bbx24bbx25elf3* seedlings grown at 22°C for six days or transferred to 27°C for 24 hours and harvested at ZT23. Histone H3 was used as a loading control and the relative levels of PIF4 protein normalized to Histone H3 are shown underneath each immunoblot.

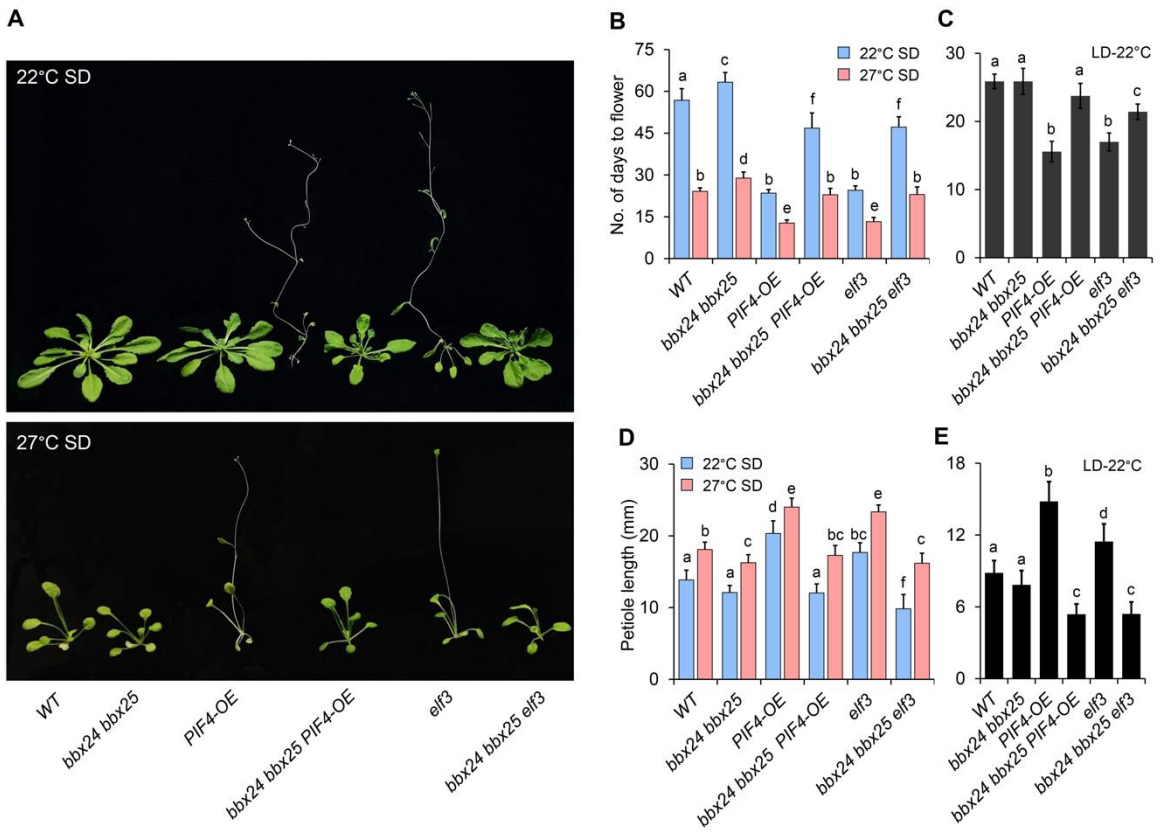

Figure 8. ELF3-BBX24/BBX25-PIF4 module controls the thermosensory flowering and petiole growth in Arabidopsis.

(**A**) Representative images of adult plants of WT, *bbx24bbx25*, PIF4-OE, bbx24bbx25PIF4-OE, *elf3* and *bbx24bbx25elf3* grown at 22°C SD and 27°C SD conditions for 30 days and 22 days, respectively.

(**B** and **C**) The flowering time of various genotypes indicated in A grown at 22°C and 27°C under SD (B) or at 22°C in LD (C) photoperiods.

(**D** and **E**) Petiole length measurement (mean ± SD; n ≥15) of genotypes indicated in A at 22°C (18 days old) and 27°C (15 days old) under SD (D) or at 22°C (18 days old) in LD (E) photoperiods.

In B and D, different letters denote statistically significant differences between the samples (Two-way ANOVA followed by Tukey's post hoc test, $p < 0.05$). In C and E, different letters depict statistically significant differences between the samples (One-way ANOVA followed by Tukey's post hoc test).

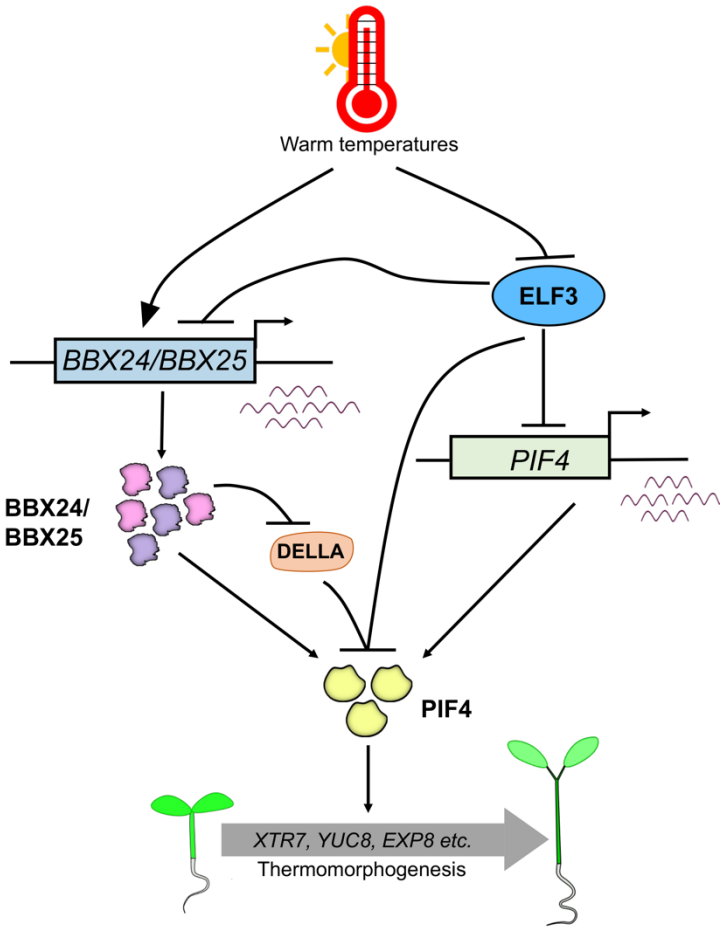

Figure 10. The molecular model depicting BBX24/BBX25-mediated regulation of thermosensory growth.

The model shows the molecular mechanism by which BBX24/BBX25 promote thermosensory growth in Arabidopsis. Warm temperatures promote *BBX24*/*BBX25* transcription and protein accumulation, enhancing PIF4 protein stability and promoting thermomorphogenesis. Parallelly, the warm temperature-mediated release of transcriptional repression of *BBX24* and *BBX25* by ELF3 and

destabilization of DELLA protein RGA by BBX24/BBX25 further amplifying the PIF4-mediated signaling output and resulting in a robust thermomorphogenic response.

Parsed Citations

Bai, M., Sun, J., Liu, J., Ren, H., Wang, K., Wang, Y., Wang, C., and Dehesh, K. (2019). The B-box protein BBX19 suppresses seed germination via induction of ABI5. Plant J 99, 1192-1202.
Google Scholar: Author Only Title Only Author and Title

Blanco-Tourinan, N., Legris, M., Minguet, E.G., Costigliolo-Rojas, C., Nohales, M.A., Iniesto, E., Garcia-Leomicronn, M., Pacin, M., Heucken, N., Blomeier, T., Locascio, A., Cerny, M., Esteve-Bruna, D., Diez-Diaz, M., Brzobohaty, B., Frerigmann, H., Zurbriggen, M.D., Kay, S.A., Rubio, V., Blazquez, M.A., Casal, J.J., and Alabadi, D. (2020). COP1 destabilizes DELLA proteins in Arabidopsis. Proc Natl Acad Sci U S A 117, 13792-13799.
Google Scholar: Author Only Title Only Author and Title

Blanco-Touriñán, N., Legris, M., Minguet, E.G., Costigliolo-Rojas, C., Nohales, M.A., Iniesto, E., García-León, M., Pacín, M., Heucken, N., Blomeier, T., Locascio, A., Černý, M., Esteve-Bruna, D., Díez-Díaz, M., Brzobohatý, B., Frerigmann, H., Zurbriggen, M.D., Kay, S.A., Rubio, V., Blázquez, M.A., Casal, J.J., and Alabadí, D. (2020). COP1 destabilizes DELLA proteins in Arabidopsis. Proc Natl Acad Sci U S A 117, 13792-13799.
Google Scholar: Author Only Title Only Author and Title

Box, M.S., Huang, B.E., Domijan, M., Jaeger, K.E., Khattak, A.K., Yoo, S.J., Sedivy, E.L., Jones, D.M., Hearn, T.J., Webb, A.A.R., Grant, A., Locke, J.C.W., and Wigge, P.A. (2015). ELF3 controls thermoresponsive growth in Arabidopsis. Curr Biol 25, 194-199.
Google Scholar: Author Only Title Only Author and Title

Buelbuel, S., Sakuraba, Y., Sedaghatmehr, M., Watanabe, M., Hoefgen, R., Balazadeh, S., and Mueller-Roeber, B. (2023). Arabidopsis BBX14 negatively regulates nitrogen starvation- and dark-induced leaf senescence. Plant J 116, 251-268.
Google Scholar: Author Only Title Only Author and Title

Burko, Y., Willige, B.C., Seluzicki, A., Novák, O., Ljung, K., and Chory, J. (2022). PIF7 is a master regulator of thermomorphogenesis in shade. Nat Commun 13, 4942.
Google Scholar: Author Only Title Only Author and Title

Burroughs, C.H., Montes, C.M., Moller, C.A., Mitchell, N.G., Michael, A.M., Peng, B., Kimm, H., Pederson, T.L., Lipka, A.E., Bernacchi, C.J., Guan, K., and Ainsworth, E.A. (2023). Reductions in leaf area index, pod production, seed size, and harvest index drive yield loss to high temperatures in soybean. J Exp Bot 74, 1629-1641.
Google Scholar: Author Only Title Only Author and Title

Bursch, K., Toledo-Ortiz, G., Pireyre, M., Lohr, M., Braatz, C., and Johansson, H. (2020). Identification of BBX proteins as rate-limiting cofactors of HY5. Nature Plants 6, 921-+.
Google Scholar: Author Only Title Only Author and Title

Casal, J.J., and Questa, J.I. (2018). Light and temperature cues: multitasking receptors and transcriptional integrators. New Phytol 217, 1029-1034.
Google Scholar: Author Only Title Only Author and Title

Casal, J.J., and Balasubramanian, S. (2019). Thermomorphogenesis. Annu Rev Plant Biol 70, 321-346.
Google Scholar: Author Only Title Only Author and Title

Chow, B.Y., Helfer, A., Nusinow, D.A., and Kay, S.A. (2012). ELF3 recruitment to the PRR9 promoter requires other Evening Complex members in the Arabidopsis circadian clock. Plant Signal Behav 7, 170-173.
Google Scholar: Author Only Title Only Author and Title

Chung, B.Y.W., Balcerowicz, M., Di Antonio, M., Jaeger, K.E., Geng, F., Franaszek, K., Marriott, P., Brierley, I., Firth, A.E., and Wigge, P.A. (2020). An RNA thermoswitch regulates daytime growth in Arabidopsis. Nat Plants 6, 522-532.
Google Scholar: Author Only Title Only Author and Title

Crawford, A.J., McLachlan, D.H., Hetherington, A.M., and Franklin, K.A. (2012). High temperature exposure increases plant cooling capacity. Curr Biol 22, R396-397.
Google Scholar: Author Only Title Only Author and Title

Crocco, C.D., Locascio, A., Escudero, C.M., Alabadí, D., Blázquez, M.A., and Botto, J.F. (2015a). The transcriptional regulator BBX24 impairs DELLA activity to promote shade avoidance in Arabidopsis thaliana. Nat Commun 6, 6202.
Google Scholar: Author Only Title Only Author and Title

Crocco, C.D., Locascio, A., Escudero, C.M., Alabadi, D., Blazquez, M.A., and Botto, J.F. (2015b). The transcriptional regulator BBX24 impairs DELLA activity to promote shade avoidance in Arabidopsis thaliana. Nat Commun 6, 6202.
Google Scholar: Author Only Title Only Author and Title

Datta, S., Johansson, H., Hettiarachchi, C., Irigoyen, M.L., Desai, M., Rubio, V., and Holm, M. (2008). LZF1/SALT TOLERANCE HOMOLOG3, an Arabidopsis B-box protein involved in light-dependent development and gene expression, undergoes COP1-mediated ubiquitination. Plant Cell 20, 2324-2338.
Google Scholar: Author Only Title Only Author and Title

de Lucas, M., Davière, J.-M., Rodríguez-Falcón, M., Pontin, M., Iglesias-Pedraz, J.M., Lorrain, S., Fankhauser, C., Blázquez, M.A., Titarenko, E., and Prat, S. (2008a). A molecular framework for light and gibberellin control of cell elongation. Nature 451, 480-484.
Google Scholar: Author Only Title Only Author and Title

de Lucas, M., Daviere, J.M., Rodriguez-Falcon, M., Pontin, M., Iglesias-Pedraz, J.M., Lorrain, S., Fankhauser, C., Blazquez, M.A., Titarenko, E., and Prat, S. (2008b). A molecular framework for light and gibberellin control of cell elongation. Nature 451, 480-484.
Google Scholar: Author Only Title Only Author and Title

Delker, C., Quint, M., and Wigge, P.A. (2022). Recent advances in understanding thermomorphogenesis signaling. Curr Opin Plant Biol 68, 102231.
Google Scholar: Author Only Title Only Author and Title

Ding, L., Wang, S., Song, Z.T., Jiang, Y., Han, J.J., Lu, S.J., Li, L., and Liu, J.X. (2018). Two B-Box Domain Proteins, BBX18 and BBX23, Interact with ELF3 and Regulate Thermomorphogenesis in Arabidopsis. Cell Rep 25, 1718-1728 e1714.
Google Scholar: Author Only Title Only Author and Title

Dixon, L.E., Knox, K., Kozma-Bognar, L., Southern, M.M., Pokhilko, A., and Millar, A.J. (2011). Temporal Repression of Core Circadian Genes Is Mediated through EARLY FLOWERING 3 in. Current Biology 21, 120-125.
Google Scholar: Author Only Title Only Author and Title

Favero, D.S., Kawamura, A., Shibata, M., Takebayashi, A., Jung, J.H., Suzuki, T., Jaeger, K.E., Ishida, T., Iwase, A., Wigge, P.A., Neff, M.M., and Sugimoto, K. (2020). AT-Hook Transcription Factors Restrict Petiole Growth by Antagonizing PIFs. Curr Biol 30, 1454-1466 e1456.
Google Scholar: Author Only Title Only Author and Title

Feng, S., Martinez, C., Gusmaroli, G., Wang, Y., Zhou, J., Wang, F., Chen, L., Yu, L., Iglesias-Pedraz, J.M., Kircher, S., Schäfer, E., Fu, X., Fan, L.-M., and Deng, X.W. (2008). Coordinated regulation of Arabidopsis thaliana development by light and gibberellins. Nature 451, 475-479.
Google Scholar: Author Only Title Only Author and Title

Fiorucci, A.S., Galvão, V.C., Ince, Y., Boccaccini, A., Goyal, A., Allenbach Petrolati, L., Trevisan, M., and Fankhauser, C. (2020). PHYTOCHROME INTERACTING FACTOR 7 is important for early responses to elevated temperature in Arabidopsis seedlings. New Phytol 226, 50-58.
Google Scholar: Author Only Title Only Author and Title

Franklin, K.A., Toledo-Ortiz, G., Pyott, D.E., and Halliday, K.J. (2014). Interaction of light and temperature signalling. J Exp Bot 65, 2859-2871.
Google Scholar: Author Only Title Only Author and Title

Franklin, K.A., Lee, S.H., Patel, D., Kumar, S.V., Spartz, A.K., Gu, C., Ye, S., Yu, P., Breen, G., Cohen, J.D., Wigge, P.A., and Gray, W.M. (2011). Phytochrome-interacting factor 4 (PIF4) regulates auxin biosynthesis at high temperature. Proc Natl Acad Sci U S A 108, 20231-20235.
Google Scholar: Author Only Title Only Author and Title

Gangappa, S.N., and Botto, J.F. (2014). The BBX family of plant transcription factors. Trends in Plant Science 19, 460-470.
Google Scholar: Author Only Title Only Author and Title

Gangappa, S.N., and Kumar, S.V. (2017). DET1 and HY5 Control PIF4-Mediated Thermosensory Elongation Growth through Distinct Mechanisms. Cell Rep 18, 344-351.
Google Scholar: Author Only Title Only Author and Title

Gangappa, S.N., Crocco, C.D., Johansson, H., Datta, S., Hettiarachchi, C., Holm, M., and Botto, J.F. (2013). The Arabidopsis B-BOX protein BBX25 interacts with HY5, negatively regulating BBX22 expression to suppress seedling photomorphogenesis. Plant Cell 25, 1243-1257.
Google Scholar: Author Only Title Only Author and Title

Gray, W.M., Ostin, A., Sandberg, G., Romano, C.P., and Estelle, M. (1998). High temperature promotes auxin-mediated hypocotyl elongation in Arabidopsis. Proc Natl Acad Sci U S A 95, 7197-7202.
Google Scholar: Author Only Title Only Author and Title

Huang, Y., Xiong, H., Xie, Y., Lyu, S., Miao, T., Li, T., Lyu, G., and Li, S. (2022). BBX24 Interacts with DELLA to Regulate UV-B-Induced Photomorphogenesis in Arabidopsis thaliana. Int J Mol Sci 23.
Google Scholar: Author Only Title Only Author and Title

Huq, E., and Quail, P.H. (2002). PIF4, a phytochrome-interacting bHLH factor, functions as a negative regulator of phytochrome B signaling in Arabidopsis. EMBO J 21, 2441-2450.
Google Scholar: Author Only Title Only Author and Title

Hwang, G., Park, J., Kim, S., Park, J., Seo, D., and Oh, E. (2021). Overexpression of BBX18 Promotes Thermomorphogenesis Through the PRR5-PIF4 Pathway. Front Plant Sci 12, 782352.

Google Scholar: Author Only Title Only Author and Title

Ibanez, C., Delker, C., Martinez, C., Burstenbinder, K., Janitza, P., Lippmann, R., Ludwig, W., Sun, H., James, G.V., Klecker, M., Grossjohann, A., Schneeberger, K., Prat, S., and Quint, M. (2018). Brassinosteroids Dominate Hormonal Regulation of Plant Thermomorphogenesis via BZR1. Curr Biol 28, 303-310 e303.
Google Scholar: Author Only Title Only Author and Title

Jiang, L., Wang, Y., Li, Q.F., Bjorn, L.O., He, J.X., and Li, S.S. (2012). Arabidopsis STO/BBX24 negatively regulates UV-B signaling by interacting with COP1 and repressing HY5 transcriptional activity. Cell Res 22, 1046-1057.
Google Scholar: Author Only Title Only Author and Title

Job, N., Lingwan, M., Masakapalli, S.K., and Datta, S. (2022). Transcription factors BBX11 and HY5 interdependently regulate the molecular and metabolic responses to UV-B. Plant Physiol 189, 2467-2480.
Google Scholar: Author Only Title Only Author and Title

Job, N., Yadukrishnan, P., Bursch, K., Datta, S., and Johansson, H. (2018). Two B-Box Proteins Regulate Photomorphogenesis by Oppositely Modulating HY5 through their Diverse C-Terminal Domains. Plant Physiol 176, 2963-2976.
Google Scholar: Author Only Title Only Author and Title

Jung, J.H., Barbosa, A.D., Hutin, S., Kumita, J.R., Gao, M., Derwort, D., Silva, C.S., Lai, X., Pierre, E., Geng, F., Kim, S.B., Baek, S., Zubieta, C., Jaeger, K.E., and Wigge, P.A. (2020). A prion-like domain in ELF3 functions as a thermosensor in Arabidopsis. Nature 585, 256-260.
Google Scholar: Author Only Title Only Author and Title

Jung, J.H., Domijan, M., Klose, C., Biswas, S., Ezer, D., Gao, M.J., Khattak, A.K., Box, M.S., Charoensawan, V., Cortijo, S., Kumar, M., Grant, A., Locke, J.C.W., Schäfer, E., Jaeger, K.E., and Wigge, P.A. (2016). Phytochromes function as thermosensors in. Science 354, 886-889.
Google Scholar: Author Only Title Only Author and Title

Khanna, R., Kronmiller, B., Maszle, D.R., Coupland, G., Holm, M., Mizuno, T., and Wu, S.H. (2009). The Arabidopsis B-box zinc finger family. Plant Cell 21, 3416-3420.
Google Scholar: Author Only Title Only Author and Title

Koester, R.P., Skoneczka, J.A., Cary, T.R., Diers, B.W., and Ainsworth, E.A. (2014). Historical gains in soybean (Glycine max Merr.) seed yield are driven by linear increases in light interception, energy conversion, and partitioning efficiencies. J Exp Bot 65, 3311-3321.
Google Scholar: Author Only Title Only Author and Title

Koini, M.A., Alvey, L., Allen, T., Tilley, C.A., Harberd, N.P., Whitelam, G.C., and Franklin, K.A. (2009). High temperature-mediated adaptations in plant architecture require the bHLH transcription factor PIF4. Curr Biol 19, 408-413.
Google Scholar: Author Only Title Only Author and Title

Krahmer, J., and Fankhauser, C. (2023). Environmental Control of Hypocotyl Elongation. Annu Rev Plant Biol.
Google Scholar: Author Only Title Only Author and Title

Kumar, S.V., Lucyshyn, D., Jaeger, K.E., Alos, E., Alvey, E., Harberd, N.P., and Wigge, P.A. (2012). Transcription factor PIF4 controls the thermosensory activation of flowering. Nature 484, 242-245.
Google Scholar: Author Only Title Only Author and Title

Lee, S., Paik, I., and Huq, E. (2020). SPAs promote thermomorphogenesis by regulating the phyB-PIF4 module in Arabidopsis. Development 147.
Google Scholar: Author Only Title Only Author and Title

Legris, M., Ince, Y.C., and Fankhauser, C. (2019). Molecular mechanisms underlying phytochrome-controlled morphogenesis in plants. Nat Commun 10, 5219.
Google Scholar: Author Only Title Only Author and Title

Legris, M., Klose, C., Burgie, E.S., Rojas, C.C., Neme, M., Hiltbrunner, A., Wigge, P.A., Schafer, E., Vierstra, R.D., and Casal, J.J. (2016). Phytochrome B integrates light and temperature signals in Arabidopsis. Science 354, 897-900.
Google Scholar: Author Only Title Only Author and Title

Li, F., Sun, J., Wang, D., Bai, S., Clarke, A.K., and Holm, M. (2014). The B-box family gene STO (BBX24) in Arabidopsis thaliana regulates flowering time in different pathways. PLoS One 9, e87544.
Google Scholar: Author Only Title Only Author and Title

Li, K., Yu, R., Fan, L.-M., Wei, N., Chen, H., and Deng, X.W. (2016a). DELLA-mediated PIF degradation contributes to coordination of light and gibberellin signalling in Arabidopsis. Nature Communications 7, 11868.
Google Scholar: Author Only Title Only Author and Title

Li, K.L., Yu, R.B., Fan, L.M., Wei, N., Chen, H.D., and Deng, X.W. (2016b). DELLA-mediated PIF degradation contributes to coordination of light and gibberellin signalling in. Nature Communications 7.

Google Scholar: Author Only Title Only Author and Title

Li, N., Zhang, Y., He, Y., Wang, Y., and Wang, L. (2020). Pseudo Response Regulators Regulate Photoperiodic Hypocotyl Growth by Repressing PIF4/5 Transcription. Plant Physiol 183, 686-699.
Google Scholar: Author Only Title Only Author and Title

Lippmann, R., Babben, S., Menger, A., Delker, C., and Quint, M. (2019). Development of Wild and Cultivated Plants under Global Warming Conditions. Curr Biol 29, R1326-R1338.
Google Scholar: Author Only Title Only Author and Title

Lorrain, S., Allen, T., Duek, P.D., Whitelam, G.C., and Fankhauser, C. (2008). Phytochrome-mediated inhibition of shade avoidance involves degradation of growth-promoting bHLH transcription factors. Plant J 53, 312-323.
Google Scholar: Author Only Title Only Author and Title

Ma, D., Li, X., Guo, Y., Chu, J., Fang, S., Yan, C., Noel, J.P., and Liu, H. (2016). Cryptochrome 1 interacts with PIF4 to regulate high temperature-mediated hypocotyl elongation in response to blue light. Proc Natl Acad Sci U S A 113, 224-229.
Google Scholar: Author Only Title Only Author and Title

Meroni, G., and Diez-Roux, G. (2005). TRIM/RBCC, a novel class of 'single protein RING finger' E3 ubiquitin ligases. Bioessays 27, 1147-1157.
Google Scholar: Author Only Title Only Author and Title

Nakamura, S., Mano, S., Tanaka, Y., Ohnishi, M., Nakamori, C., Araki, M., Niwa, T., Nishimura, M., Kaminaka, H., Nakagawa, T., Sato, Y., and Ishiguro, S. (2010). Gateway Binary Vectors with the Bialaphos Resistance Gene, as a Selection Marker for Plant Transformation. Biosci Biotech Bioch 74, 1315-1319.
Google Scholar: Author Only Title Only Author and Title

Nieto, C., Lopez-Salmeron, V., Daviere, J.M., and Prat, S. (2015). ELF3-PIF4 interaction regulates plant growth independently of the Evening Complex. Curr Biol 25, 187-193.
Google Scholar: Author Only Title Only Author and Title

Nusinow, D.A., Helfer, A., Hamilton, E.E., King, J.J., Imaizumi, T., Schultz, T.F., Farre, E.M., and Kay, S.A. (2011). The ELF4-ELF3-LUX complex links the circadian clock to diurnal control of hypocotyl growth. Nature 475, 398-402.
Google Scholar: Author Only Title Only Author and Title

Oh, E., Zhu, J.Y., and Wang, Z.Y. (2012). Interaction between BZR1 and PIF4 integrates brassinosteroid and environmental responses. Nat Cell Biol 14, 802-809.
Google Scholar: Author Only Title Only Author and Title

Park, Y.-J., Kim, J.Y., Lee, J.-H., Lee, B.-D., Paek, N.-C., and Park, C.-M. (2020). GIGANTEA Shapes the Photoperiodic Rhythms of Thermomorphogenic Growth in Arabidopsis. Molecular Plant 13, 459-470.
Google Scholar: Author Only Title Only Author and Title

Park, Y.J., Kim, J.Y., and Park, C.M. (2022). SMAX1 potentiates phytochrome B-mediated hypocotyl thermomorphogenesis. Plant Cell 34, 2671-2687.
Google Scholar: Author Only Title Only Author and Title

Park, Y.J., Lee, H.J., Ha, J.H., Kim, J.Y., and Park, C.M. (2017). COP1 conveys warm temperature information to hypocotyl thermomorphogenesis. New Phytol 215, 269-280.
Google Scholar: Author Only Title Only Author and Title

Peng, S., Huang, J., Sheehy, J.E., Laza, R.C., Visperas, R.M., Zhong, X., Centeno, G.S., Khush, G.S., and Cassman, K.G. (2004). Rice yields decline with higher night temperature from global warming. Proc Natl Acad Sci U S A 101, 9971-9975.
Google Scholar: Author Only Title Only Author and Title

Podolec, R., Wagnon, T.B., Leonardelli, M., Johansson, H., and Ulm, R. (2022). Arabidopsis B-box transcription factors BBX20-22 promote UVR8 photoreceptor-mediated UV-B responses. Plant J 111, 422-439.
Google Scholar: Author Only Title Only Author and Title

Qiu, Y., Li, M., Kim, R.J., Moore, C.M., and Chen, M. (2019). Daytime temperature is sensed by phytochrome B in Arabidopsis through a transcriptional activator HEMERA. Nat Commun 10, 140.
Google Scholar: Author Only Title Only Author and Title

Qiu, Y., Pasoreck, E.K., Yoo, C.Y., He, J., Wang, H., Bajracharya, A., Li, M., Larsen, H.D., Cheung, S., and Chen, M. (2021). RCB initiates Arabidopsis thermomorphogenesis by stabilizing the thermoregulator PIF4 in the daytime. Nat Commun 12, 2042.
Google Scholar: Author Only Title Only Author and Title

Quint, M., Delker, C., Franklin, K.A., Wigge, P.A., Halliday, K.J., and van Zanten, M. (2016). Molecular and genetic control of plant thermomorphogenesis. Nat Plants 2, 15190.
Google Scholar: Author Only Title Only Author and Title

Quint, M., Delker, C., Balasubramanian, S., Balcerowicz, M., Casal, J.J., Castroverde, C.D.M., Chen, M., Chen, X., De Smet, I., Fankhauser, C., Franklin, K.A., Halliday, K.J., Hayes, S., Jiang, D., Jung, J.H., Kaiserli, E., Kumar, S.V., Maag, D., Oh, E., Park, C.M., Penfield, S., Perrella, G., Prat, S., Reis, R.S., Wigge, P.A., Willige, B.C., and van Zanten, M. (2023). 25 Years of thermomorphogenesis research: milestones and perspectives. Trends Plant Sci 28, 1098-1100.
Google Scholar: Author Only Title Only Author and Title

Saura-Sanchez, M., Chiriotto, T.S., Cascales, J., Gomez-Ocampo, G., Hernandez-Garcia, J., Li, Z., Pruneda-Paz, J.L., Blazquez, M.A., and Botto, J.F. (2023). BBX24 Interacts with JAZ3 to Promote Growth by Reducing DELLA Activity in Shade Avoidance. Plant Cell Physiol 64, 474-485.
Google Scholar: Author Only Title Only Author and Title

Silva, C.S., Nayak, A., Lai, X., Hutin, S., Hugouvieux, V., Jung, J.H., Lopez-Vidriero, I., Franco-Zorrilla, J.M., Panigrahi, K.C.S., Nanao, M.H., Wigge, P.A., and Zubieta, C. (2020). Molecular mechanisms of Evening Complex activity in Arabidopsis. Proc Natl Acad Sci U S A 117, 6901-6909.
Google Scholar: Author Only Title Only Author and Title

Song, Z.Q., Bian, Y.T., Liu, J.J., Sun, Y., and Xu, D. (2020). B-box proteins: Pivotal players in light-mediated development in plants. Journal of Integrative Plant Biology 62, 1293-1309.
Google Scholar: Author Only Title Only Author and Title

Stavang, J.A., Gallego-Bartolome, J., Gomez, M.D., Yoshida, S., Asami, T., Olsen, J.E., Garcia-Martinez, J.L., Alabadi, D., and Blazquez, M.A. (2009). Hormonal regulation of temperature-induced growth in Arabidopsis. Plant J 60, 589-601.
Google Scholar: Author Only Title Only Author and Title

Sun, J., Qi, L., Li, Y., Chu, J., and Li, C. (2012). PIF4-mediated activation of YUCCA8 expression integrates temperature into the auxin pathway in regulating arabidopsis hypocotyl growth. PLoS Genet 8, e1002594.
Google Scholar: Author Only Title Only Author and Title

Sun, Q., Wang, S., Xu, G., Kang, X., Zhang, M., and Ni, M. (2019). SHB1 and CCA1 interaction desensitizes light responses and enhances thermomorphogenesis. Nat Commun 10, 3110.
Google Scholar: Author Only Title Only Author and Title

Tan, W., Chen, J., Yue, X., Chai, S., Liu, W., Li, C., Yang, F., Gao, Y., Gutiérrez Rodríguez, L., Resco de Dios, V., Zhang, D., and Yao, Y. (2023a). The heat response regulators HSFA1s promote Arabidopsis thermomorphogenesis via stabilizing PIF4 during the day. Sci Adv 9, eadh1738.
Google Scholar: Author Only Title Only Author and Title

Tan, W., Chen, J., Yue, X., Chai, S., Liu, W., Li, C., Yang, F., Gao, Y., Gutierrez Rodriguez, L., Resco de Dios, V., Zhang, D., and Yao, Y. (2023b). The heat response regulators HSFA1s promote Arabidopsis thermomorphogenesis via stabilizing PIF4 during the day. Sci Adv 9, eadh1738.
Google Scholar: Author Only Title Only Author and Title

Torok, M., and Etkin, L.D. (2001). Two B or not two B? Overview of the rapidly expanding B-box family of proteins. Differentiation 67, 63-71.
Google Scholar: Author Only Title Only Author and Title

Tripathi, P., Carvallo, M., Hamilton, E.E., Preuss, S., and Kay, S.A. (2017). Arabidopsis B-BOX32 interacts with CONSTANS-LIKE3 to regulate flowering. Proc Natl Acad Sci U S A 114, 172-177.
Google Scholar: Author Only Title Only Author and Title

Vaishak, K.P., Yadukrishnan, P., Bakshi, S., Kushwaha, A.K., Ramachandran, H., Job, N., Babu, D., and Datta, S. (2019). The B-box bridge between light and hormones in plants. J Photoch Photobio B 191, 164-174.
Google Scholar: Author Only Title Only Author and Title

Wang, C.Q., Guthrie, C., Sarmast, M.K., and Dehesh, K. (2014). BBX19 interacts with CONSTANS to repress FLOWERING LOCUS T transcription, defining a flowering time checkpoint in Arabidopsis. Plant Cell 26, 3589-3602.
Google Scholar: Author Only Title Only Author and Title

Wang, C.Q., Sarmast, M.K., Jiang, J., and Dehesh, K. (2015). The Transcriptional Regulator BBX19 Promotes Hypocotyl Growth by Facilitating COP1-Mediated EARLY FLOWERING3 Degradation in Arabidopsis. Plant Cell 27, 1128-1139.
Google Scholar: Author Only Title Only Author and Title

Xu, D., Jiang, Y., Li, J., Lin, F., Holm, M., and Deng, X.W. (2016). BBX21, an Arabidopsis B-box protein, directly activates HY5 and is targeted by COP1 for 26S proteasome-mediated degradation. Proc Natl Acad Sci U S A 113, 7655-7660.
Google Scholar: Author Only Title Only Author and Title

Xu, D., Li, J., Gangappa, S.N., Hettiarachchi, C., Lin, F., Andersson, M.X., Jiang, Y., Deng, X.W., and Holm, M. (2014a). Convergence of Light and ABA signaling on the ABI5 promoter. PLoS Genet 10, e1004197.
Google Scholar: Author Only Title Only Author and Title

Xu, K., Huang, X., Wu, M., Wang, Y., Chang, Y., Liu, K., Zhang, J., Zhang, Y., Zhang, F., Yi, L., Li, T., Wang, R., Tan, G., and Li, C. (2014b). A rapid, highly efficient and economical method of Agrobacterium-mediated in planta transient transformation in living onion epidermis. PLoS One 9, e83556.
Google Scholar: Author Only Title Only Author and Title

Yamaguchi, N., Winter, C.M., Wu, M.F., Kwon, C.S., William, D.A., and Wagner, D. (2014). PROTOCOLS: Chromatin Immunoprecipitation from Arabidopsis Tissues. Arabidopsis Book 12, e0170.
Google Scholar: Author Only Title Only Author and Title

Yuan, L., Yu, Y.J., Liu, M.M., Song, Y., Li, H.M., Sun, J.Q., Wang, Q., Xie, Q.G., Wang, L., and Xu, X.D. (2021). BBX19 fine-tunes the circadian rhythm by interacting with PSEUDO-RESPONSE REGULATOR proteins to facilitate their repressive effect on morning-phased clock genes. Plant Cell 33, 2602-2617.
Google Scholar: Author Only Title Only Author and Title

Zhao, C., Liu, B., Piao, S., Wang, X., Lobell, D.B., Huang, Y., Huang, M., Yao, Y., Bassu, S., Ciais, P., Durand, J.L., Elliott, J., Ewert, F., Janssens, I.A., Li, T., Lin, E., Liu, Q., Martre, P., Muller, C., Peng, S., Penuelas, J., Ruane, A.C., Wallach, D., Wang, T., Wu, D., Liu, Z., Zhu, Y., Zhu, Z., and Asseng, S. (2017). Temperature increase reduces global yields of major crops in four independent estimates. Proc Natl Acad Sci U S A 114, 9326-9331.
Google Scholar: Author Only Title Only Author and Title

Zhao, H., and Bao, Y. (2021). PIF4: Integrator of light and temperature cues in plant growth. Plant Sci 313, 111086.
Google Scholar: Author Only Title Only Author and Title

Zhao, X., Heng, Y., Wang, X., Deng, X.W., and Xu, D. (2020). A Positive Feedback Loop of BBX11-BBX21-HY5 Promotes Photomorphogenic Development in Arabidopsis. Plant Commun 1, 100045.
Google Scholar: Author Only Title Only Author and Title

Zhu, J.Y., Oh, E., Wang, T., and Wang, Z.Y. (2016). TOC1-PIF4 interaction mediates the circadian gating of thermoresponsive growth in Arabidopsis. Nat Commun 7, 13692.
Google Scholar: Author Only Title Only Author and Title